Int. J. Electrochem. Sci., 11 **(2016)** 506 - 534

International Journal of
ELECTROCHEMICAL
SCIENCE
www.electrochemsci.org

Review

Development of Fabrication Methods and Performance Analysis of Various Electrodes in Direct Methanol Fuel Cells (DMFCs)

Rasu Ramachandran[1], *George peter Gnana kumar*[2], *Shen-Ming Chen*[3,*]

[1]Department of Chemistry, The Madura College, Vidya Nagar, Madurai – 625 011, Tamil Nadu, India.
[2]Department of Physical Chemistry, School of Chemistry, Madurai Kamaraj University, Madurai-625 021, Tamil Nadu, India.
[3]Electroanalysis and Bioelectrochemistry Lab, Department of Chemical Engineering and Biotechnology, National Taipei University of Technology, No.1, Section 3, Chung-Hsiao East Road, Taipei 106.Taiwan (ROC).
[*]E-mail: smchen78@ms15.hinet.net

Received: 2 September 2015 / *Accepted:* 26 October 2015 / *Published:* 1 December 2015

The significance of research methodology and the development of different nanostructured electrode catalysts for the study of direct methanol fuel cells (DMFCs) applications. In this article which has explained that the multi-disciplinary electrode materials (Carbon fiber, MWCNT, graphene oxide, metal nanoparticles, bimetallic nanoparticles, metal oxides, conducting polymers and nano composites etc.), Analyses and electro analytical technologies were applied in a variety of scientific communities. These kinds of fabricating electrode catalysts have opened the possibilities of the discussed morphological properties (Size and shape of the particles) and electrochemical parameters like operating conditions, power density, BET surface area and electrode performance etc. In addition that, we have more focus on the simple fabrication techniques, compact design, low-cost electrode catalyst, reliability, stability and improved their energy density of DMFCs.

Keywords: Electrocatalysts, Effect of parameters, Electrochemical techniques, Methanol oxidation, Direct methanol fuel cells.

1. INTRODUCTION

Direct methanol fuel cells (DMFCs) are promising alternative for power generation technologies; they transformed chemical energy into electrical power energy due to the simplicity in device fabrication, high power density and good portability [1-4]. The different carbon based electrode materials such as carbon fiber, fullerene and MWCNT electrodes have tremendously improved their (Physical and chemical properties) wide range of applications [5-6]. This article can reflect the three

generations (Past and future) of different electrode catalysts were used in DMFC analysis. The electrocatalytic activity of Au-Pt alloy particle modified with cauliflower-like microstructure of Pt/Au ratio electrodepostion on indium tin oxide (ITO). The electrochemical parameters have been optimized during the electrolysis of methanol oxidation. Such as electrochemical surface area, peak current density and electron transfer coefficient (α) [7]. A facile synthesis of carbon supported pseudo-core@shell PdCu@Pt nano catalyst has been explored extensively studied for DMFCs, such PdCu@Pt/C composite may lead to the development of enhanced specific activity and large-scale production [8]. Developing of PtRu catalyst can modified with three different carbon supported electrode (Vulcan, graphitized carbon nanofiber (GNF) and few-walled carbon nanotube (FWCNT)) with controlled the highest open circuit voltage (OCV) and current densities in DMFC applications. The non-optimized PtRu/GNF MEAs exhibit good stability and novel carbon supported catalyst for stable fuel components [9]. Samant *et al* [10] proposed appropriating synthesis of Pt and Pt-Ru catalyst using HY zeolite supported electrodes with an anodic oxidation of methanol in an acidic condition. The zeolite contained electrode catalyst displayed a significant enhanced electrocatalytic activity in the following orders like HY<Pt/C<Pt(HY)<Pt-Ru/C<Pt-Ru(HY). Although several reviews have been used to investigate their different electrode materials, fabrication techniques, different environmental conditions and optimized their mechanical aspects of methanol oxidation in DMFCs applications [11-15]. Hollow graphitic carbon spheres (HGCSs) has been successfully synthesized through carbonization of hollow polymer spheres obtained by the polymerization of core-shell structured pyrrole micelles. In addition that, the catalyst commonly used in DMFCs application and observed/improved their electrocatalytic activity of HGCSs [16]. Especially, methanol oxidation fuel cell catalyst was prepared in a way that highly catalytic active Pt supported on sulphated SnO_2/MWCNT (S-SnO_2/MWCNT) composite provides a better catalytic activity and CO tolerance for fuel cell applications [17]. Abida et al [18] found that hydrogeno titanates (HTNs) were prepared from TiO_2 powder by hydrothermal (At 30º C for 20 hrs) method. The Pt/HTNs catalyst further annealed at 500º C under air atmospheric conditions for 2 hrs. The nitrogen adsorption-desorption isotherm of multi-walled nano tubular structure, the BET surface area value significantly increased from 43 to 246 m^2 g^{-1}. In addition, the nano porous structure of CuO/ZnO/$Al2O_3$ allows for enabling better electrocatalytic performance of methanol oxidation and increased their BET surface area values [19]. The different morphological electrode materials provided with various potentially electrochemical applications in energy storage devices (Super capacitor and solar cell) [20-22], pesticide sensor [23] and biosensors [24, 25] respectively. Palladium nanoparticle supported carbon black (XC-72R) and TiO_2/C electro catalysts have been synthesized by organic colloidal method. The electrode materials were optimized at 170º C and the electrochemical active surface area (ECSA) value decreased from 22 to 18 m^2 g^{-1} [26]. Similarly, a novel bamboo charcoals (BC)-supported titanium oxide/tungsten carbide (TiO_2/WC/BC) catalyst that has attracted attention for electro catalysis in DMFCs application. The resulted synergetic effects between Pt, TiO_2 and WC, BC act as the new carbon based electrode materials which taking the role of the intermediate between the other components [27].

In the present study, we have discussed about various types of preparation methods and different electrode materials for use towards methanol oxidation reactions. Subsequently, we have highlighted the size and shape of the morphological structures and the optimized electrochemical

parameters such as annealing effect, effect of morphology and BET surface. The major aim of this article has been used to investigate the mechanistic aspects, new kinds of methodology and recent invented electrode catalysts to improve their electrocatalytic performance of DMFCs and its power density values.

2. ELECTRODE CATALYSTS

2.1. Carbon based catalyst

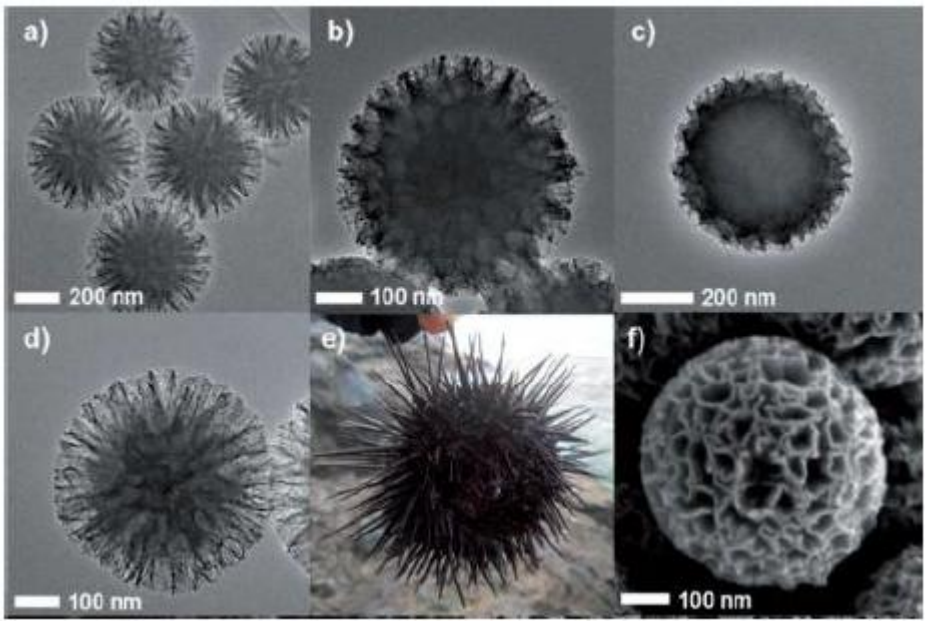

Figure 1. FHR-TEM images of (a) Silica template, (b) Silica−carbon composite after drying, (c) Silica−carbon composite after aging, (d) Sea-urchin-like three-dimensional carbon, (e) Image of sea urchin Echinometra mathae. SEM images of (f) Single sea-urchin-like three dimensional carbons and (g) Cross-section of three-dimensional carbon. ("Reprinted with permission from (*ACS catalysis* 4 (2014) 3393-3410). Copyright (2014) American Chemical Society").

One of the nitrogen doped nickel incorporated carbon nanofiber can be used for direct methanol fuel cell (DMFCs) applications. The fabricated electrode catalysts have been calcinated from nickel acetate tetrahydrate (NiAc), polyvinyl alcohol (PVA) and urea under argon conditions at 750º C. Figure.1 shows FHR-TEM a Pt supported sea-urchin-like three dimensional mesoporous carbons based materials were prepared by a nano casting method. This kind of carbon materials which can be used as an emerging catalytic activity in biomass transformation application [28]. The electroactive modified carbon ceramic platinum nanocomposite has been explored extensively for methanol and ethanol oxidation. The fabricated catalysts were exhibited long term stability and good reproducibility under ambient conditions [29]. Aarnio *et al* [30] have used three different carbon supported (Valcan, graphitized carbon nanofiber (GNF) and few-walled carbon nanofiber (FWCNT)) electrode materials fabricated with PtRu catalyst in a direct methanol fuel cell applications. The electrochemical

performance shows that, PtRu/GNF catalyst reached highest current density than PtRu/FWCNT. Similarly, the other types of four different Pt-Ru based carbon supported catalyst can be used in DMFCs, such as functionalized (HNO_3) carbon black, mesoporous carbon (CMK-3), a physical mixture of TiO_2 & carbon black and a reference carbon thermally treated in a helium atmosphere (HeTT). Especially the above kinds of catalysts, the three modified electrodes were obtained better electrocatalytic activity than the reference HeTT and also the reported highest power density values of carbon treated with HNO_3 (65 mw cm^{-2} / 300 mA cm^{-2}) catalyst at 90º C [31]. Another hybrid ordered mesoporous carbon (OMC) supported tungsten oxide composite has been synthesized by impregnation of phosphor tungstic acid (PWA) on to OMCs followed by the thermal decomposition under nitrogen atmosphere at three different temperatures. Specifically, at 500º C catalyst (Pt/OMC-WO_3-500) showed better electrocatalytic activity and significant mass-specific enhancement through methanol oxidation reaction [32]. A simple method has been the galvanostatic displacement reaction between carbon supported pseudo-core@shell with PdCu@Pt (PdCu@Pt/C) catalyst used in DMFCs. In this facile synthesis is very simple, economical, low cost and it may obtain large scale production [33]. One-dimensional carbon nanofiber supported graphite paper have been prepared by a controlled enhanced chemical vapor deposition (CVD) method and it was characterized by field emission gun scanning electron microscopy and XPS. A general observation made from cyclic voltammetry in H_2SO_4 and H_2SO_4 with methanol to estimate the electrocatalytic activity and its stability [34].

2.2. Carbon nanotube based catalyst

The preparation of a Pt supported $LaFeO_3$ nanoparticle can be modified with carbon nanotube and chitosan (GC/Pt NPs-$LaFeO_3$ NPs-CNT-CH) composite catalyst by a rapid microwave-assisted co-precipitation method, for investigating of its electrocatalytic oxidation of methanol. In addition of $LaFeO_3$ and CNT on Pt nanoparticle, the electrode surface was more porous and to enhance the catalytic performance of methanol oxidation [35]. Tsai *et al* [36] investigated the methanol oxidation using Pt supported dense carbon nanotube and ruthenium nanoparticle (Pt-Ru/CNT) catalyst by thermal vapor deposition and pulse-mode potentiostatic electrodeposition method as the electro catalyst in an 0.5 M sulphuric acid conditions. The catalyst exhibits good stability and better electrocatalytic (1038.25 A g^{-1}_{pt}) activity. Moreover, the electrochemical oxidation of methanol has been reported on a nanostructured PtRu and Pt dispersed functionalized graphene modified with functionalized multi-walled carbon nanotube (PtRu/(f-G-f-MWNT)) composite. The carbon nanotube catalyst has been electrochemically studies for the methanol oxidation by cyclic voltammetry and chronopotentiometry methods. The electrode fabrication ratios of PtRu/(50 wt % f-MWNT + 50 wt % f-G) and Pt/(50 wt % f-MWNT + 50 wt % f-G) were acting as an anode and cathode, the observed power density value of 68 mW cm^{-2} [37]. Zhao *et al* [38] reported the preparation of electro active binary composite Ni@Pd core-shell nanoparticle coated on multi-walled carbon nanotube (Ni@Pd/MWCNT). The catalyst surface was characterized by SEM analysis, in figure.1.shows that, tangled, ropes and smooth surface. The core-shell nanoparticle of MWCNT average diameter was evaluated to be 6-8 nm. The electrochemical test at methanol oxidation reaction conditions showed that

Pt/Mn_3O_4-MWCNT catalyst prepared by a simple and low cost method resulted in an electrocatalytic activity towards the methanol oxidation. Pt/Mn_3O_4-MWCNT composite, which was 1.78 times higher than that of Pt/MWCNT and 2.3 times higher than that of PtRu/MWCNT composites [39]. The anodic catalyst of Pt supported MWCNT modified with methylene blue (Pt/f_1-MWCNT) by ultraviolet irradiation method and it can be used for methanol oxidation fuel cell applications [40]. The efficient electrocatalytic properties of methanol oxidation on Pt-Ru supported carbon fiber electrode modified with single-walled carbon nanotube (CFS/SES-SWCNT/Pt-Ru) and CFE/carbon nanofiber (CNF/Pt-Ru) catalysts have been investigated by SEM and galvanostatic polarization method as shown in Fig.2. [41].

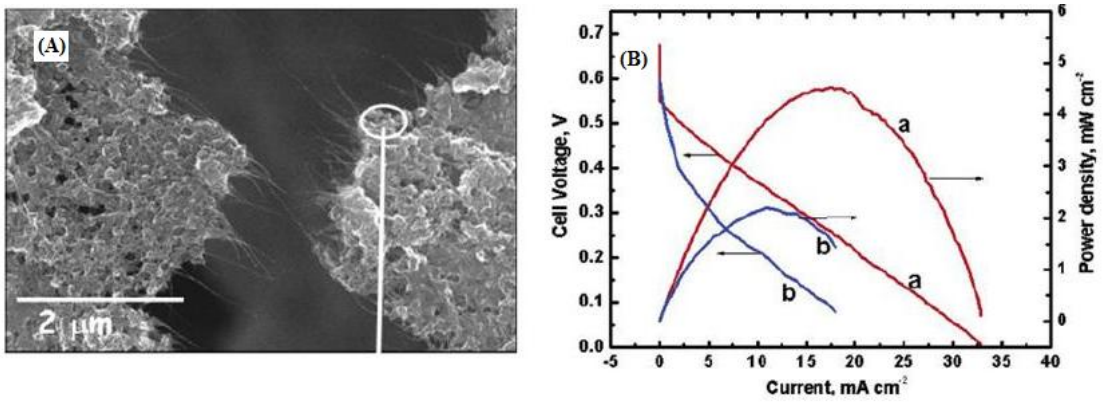

Figure 2. (A) Scanning electron micrograph showing carbon fiber electrode (CFE) deposited with SWCNT (B) Power density and galvanostatic polarization data at 25° C of an MEA prepared using (a) CFE/SES-SWCNT/Pt-Ru and (b) CFE/Carbon nano fiber/Pt-Ru anodes. The cathode for both MEAs was Pt black at 1.5 mg/cm^2 dispersed on carbon black (~2 mg/cm^2). The loading of Pt-Ru on anode electrodes was ~0.2 mg/cm^2 on ~0.5 mg/cm^2 of carbon support (SES or C nano fiber). ("Reprinted with permission from (*J. Phys. Chem. B* 110 (2006) 107-114). Copyright (2006) American Chemical Society").

2.3. Graphene based catalyst

Zhang *et al* [42] have used a simple one-pot microwave-polyol method for the fabrication of anchor platinum nanoparticle on graphene with poly(diallyldimethyl ammonium chloride) (Pt/PDDA-G). The small particle size, high concentration and well functionalized graphene supported Pt/PDDA-G catalysts were optimized better electrocatalytic activity and stability than Pt/graphene through cyclic voltammetry and chronopotentiometric techniques. Another approach has been the palladium-graphene nanocomposite from poly vinyl pyrrolidone (PVP)-functionalized graphene oxide and Pd precursor in the presence of ascorbic acid. By using morphological (TEM) and structural analysis, Pd nanoparticle was obtained in crystalline nature and the crystallized particle diameter of about 8.5 nm [43]. A simple, facile approach to prepare a two-dimensional sandwich-like platinum supported reduced graphene oxide (Pt/Mn_3O_4/RGO) nanocomposite has been explored in the enhanced electrochemical performance in methanol oxidation. In this Pt/Mn_3O_4/RGO catalyst, which can be greatly reduced the over potential, long term stability and excellent electrocatalytic activity towards the methanol

oxidation [44]. The methanol oxidation reaction has been studied on graphene nano sheets (GN) modified with Prussian blue and platinum nanoparticles (Pt/PB/GN) composite. The catalyst has been used for the high stability towards methanol oxidations and the significant enhancement of the electrocatalytic mass activity values of 445 mA mg^{-1}_{pt} [45]. Platinum supported graphene modified by CeO_2 (Pt-CeO_2/GN) hybrid was synthesized by a two-step method such as hydrothermal method and impregnation chemical reduction method. The electrocatalytic activity of the average diameter (4.1 nm) graphene modified for direct methanol fuel cell applications [46]. Zhai *et al* [47] have used Pt nano flowers supported highly ordered TiO_2 nanotube arrays (TNTs) by the modification of reduced graphene oxide (RGO) (Pt-TNTs/RGO) catalyst exhibited a remarkable and photo catalytic response of methanol (Fig.3)

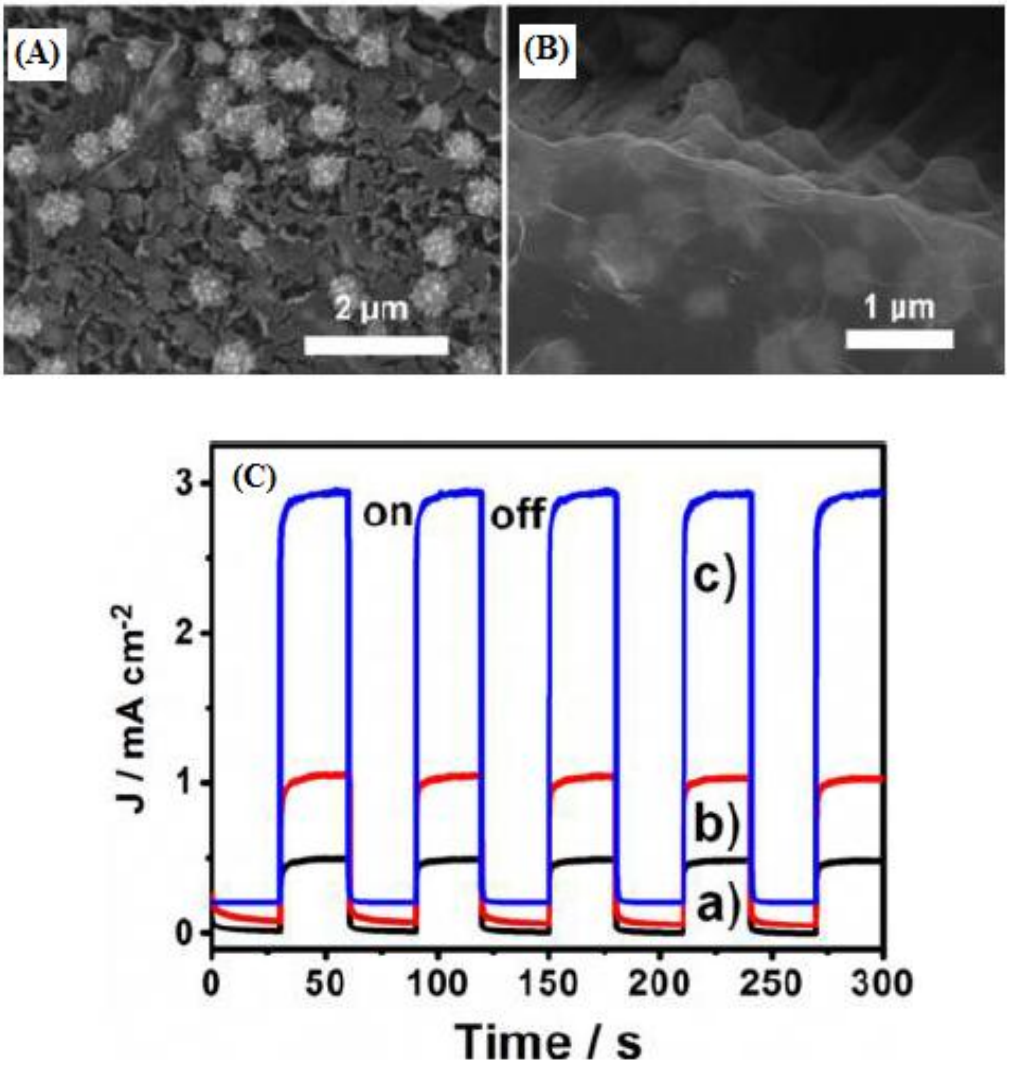

Figure 3. (A & B) SEM images of Pt-TNTs/RGO nanostructures (C) Photocurrent responses of (a) TNTs, (b) Pt-TNTs and (c) Pt-TNTs/RGO electrode under light irradiation in 1.0 M CH_3OH + 0.5 M KOH solution recorded at -0.3 V. The illumination from a Xe lamp was interrupted every 30 s. ("Reprinted with permission from (*ACS Appl. Mater. Interfaces* 6 (2014) 17753-17761). Copyright (2014) American Chemical Society").

2.4. Conducting polymer based catalyst

Jiang *et al* [48] introduced an electrochemical method to produce a Pt based free-standing poly[poly(N-vinyl carbazole)] (PPVK) as support (Pt-M/PPVK, M = Pd, Pt and Ru) electrode. This method was useful to increase the catalyst surface functional sites of Pt-M/PPVK catalyst, which was tested for fuel cell reactions. Gao *et al* performed four different carbon based electrode materials such as Pt, GCE, bare solid carbon paste electrode (sCPE) and poly(2-amino-5-mercapto-1,3,4-thiazole) (PAMT).

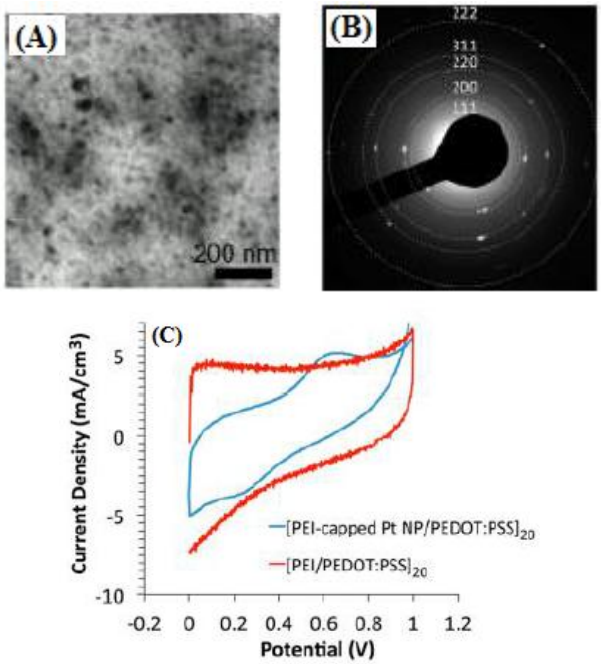

Figure 4. (A and B) TEM image and SAED of PEI-capped Pt NPs with superimposed rings indexed to FCC Pt to guide the eye (C) Cyclic voltammetry (vs Ag/AgCl) plots for methanol oxidation reaction catalyzed by a [PEI-capped Pt NPs/(PEDOT:PSS)]$_{20}$ multilayer working electrode at 0.050 V/sec in 0.1 M H_2SO_4 and 2M CH_3OH. ("Reprinted with permission from (*ACS Appl. Mater. Interfaces* 4 (2012) 3575-3583). Copyright (2012) American Chemical Society").

The combination of sCPE/PAMT catalyst showed superior electrocatalytic properties than others [49]. Wang *et al* [50] reported that a platinum micro particle interface on conducting polymer modified with nichrome matrix (Pt/PAn/Nc) catalyst by a simple and green approach method for methanol oxidation. The electrode observed anti-CO poisoning capacity, decreased the electrode cost and very simple. The polyethyleneimine-capped platinum nanoparticles (PEI-PtNPs) have been synthesized by photoreduction method and it can be characterized by TEM (Fig.4 (A) & (B)). This catalyst (PEI-PtNPs) which can be modified with conducting polymers of poly(3,4-ethylenedioxy thiophene:poly(styrene sulfonate) [(PEDOT:PSS)$^-$Na$^+$]. The catalyst [PEI-capped PtNPs/PEDOT:PSS]$_{20}$ exhibiting the best improvement of active catalyst for methanol oxidation (Fig.4C) [51]. The electrochemical preparation of Pt supported polyindole (Pt/PIn) and poly(5-

methoxy indole) (Pt/PMI) catalysts have been used for methanol oxidation. The resulted catalyst exhibits higher catalytic activity and stronger poisoning tolerance than Pt/polypyrrole/GC and Pt/GC. By applying electrochemical impedance spectroscopic (EIS) analysis, the charge-transfer resistances for methanol oxidation on Pt/Pin/GC and Pt/PMI/GC catalysts are smaller than the others [52]. Another approach has been the electro polymerization of aniline and its derivatives on pre-treated aluminium and platinum (Al/Pt) electrodes. The applied electrode potential was swept between -0.2 to 1.0 V *vs* SCE using 0.1M H_2SO_4 and 0.1M aniline. The Pt supported polyaniline matrix showed enhanced the electrocatalytic activity towards methanol oxidation reactions [53]. Radiolysis and salient synthesis aspects were viable approaches in the preparation of conducting polymer (Poly (diphenyl butadiene) (PDPB)) supported palladium nano plate (PDPB/Pd) hybrid has been used in DMFCs. The composite was developed in a real passive DMFC and the enhancement of catalytic activity [54].

2.5. Metal nanoparticle based catalyst

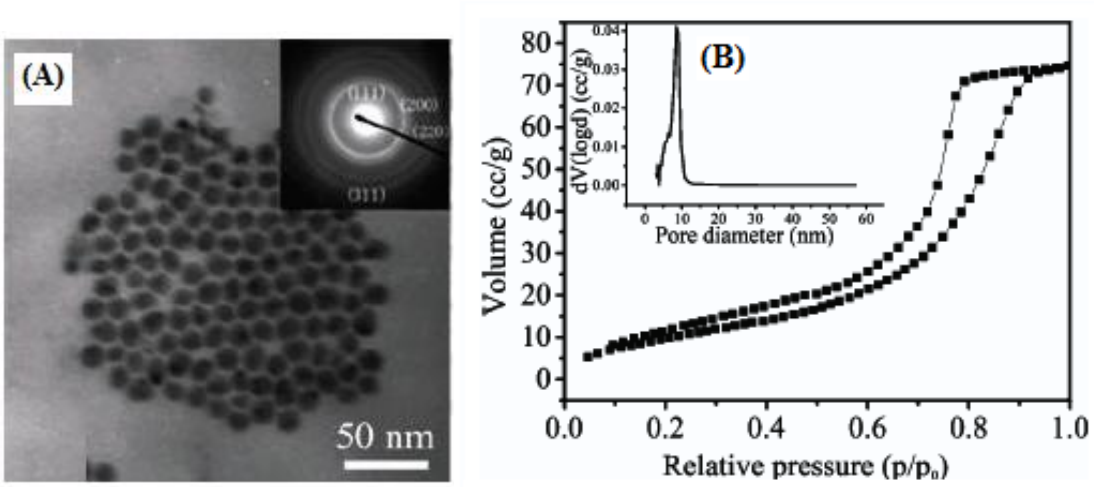

Figure 5. (A) TEM image of Pd nanoparticles obtained under nitrogen atmospheres (B) Nitrogen adsorption/desorption isotherms for the sample obtained in air atmosphere, and the inset is the corresponding BJH pore size distribution curve. ("Reprinted with permission from (*ACS Appl. Mater. Interfaces* 3 (2011) 2425-2430). Copyright (2011) American Chemical Society").

The electrocatalytic oxidation of methanol on a mono dispersed Pd nanoparticle catalyst has been reported. The morphological studies (10 nm) and BET surface area analysis (40.1 m^2 g^{-1}) have been evaluated by TEM and N_2 adsorption/desorption isotherm curve shown in Fig.5 [55]. The Volmer-Weber growth mechanism of palladium nanoparticles were synthesized on platinum electrode by pulse electro deposition containing 1mM K_2PdCl_4 in 0.1M H_2SO_4. The crystalline resulted catalyst was exhibited good electrocatalytic activity performance towards the oxidation of formic acid and methanol [56]. A novel ion exchange method for synthesis of molybdenum carbide (Mo_2C) particle incorporating on carbonized resin (C-Mo_2C) and the diameter of the Mo_2C particles can be easily controlled by Mo precursor concentrations. The synergetic effect of Pt/C-Mo_2C was obtained higher electrical current enhancement than Pt/C [57]. Sawy *et al* [58] have reported that co-electro deposition

(co-ED) of mixed iridium and platinum (Pt-Ir) thin film caused a great in electrocatalytic activity for methanol oxidation reaction. Yao *et al* [59] found by use of scanning electron microscopy that platinum nanoparticles were uniformly deposited on reducing graphene sheets. They found the catalytic activity to be depending on Pt loading in the film thickness. A novel three-dimensional N-Pt/RGO/CF catalyst showed good electrochemical properties of methanol electro oxidation reaction in alkaline conditions. The chemical vapor deposition (CVD) is advantageous over the chemical rout synthesis of silver deposited titania (Ag/TiO_2) nanocomposite thin film. Moreover, the nanocomposite has been applied the photo electrocatalytic performance of methanol oxidation reaction under simulated solar AM 1.5G irradiation conditions [60]. Hosseini *et al* [61] explored a novel and facile method for the preparation of a bimetallic (Pt-Cu) based poly(o-Anisidine) (POA) through electrodeposition on carbon paste electrode (Pt-Cu/POA/pCPE). The electrocatalytic study of methanol oxidation showed satisfactory results and low-cost preparation technique.

2.6. Bimetallic nanoparticle based catalyst

A mixture of $Ir_4(CO)_{12}/Rh_6(CO)_{16}$ has been used as the pyrrolysis method in the formation of Rh-Ir catalyst for DMFC. The electrode materials can be applied for the reduction of oxygen, hydrogen and oxidation of methanol in 0.5M H_2SO_4. The resulted new kind of catalyst showed good potential candidate to be evaluated in both anode and cathode in a reforming of polymer electrolyte membrane fuel cell (PEMFC), and as an anode applied in DMFC [62].

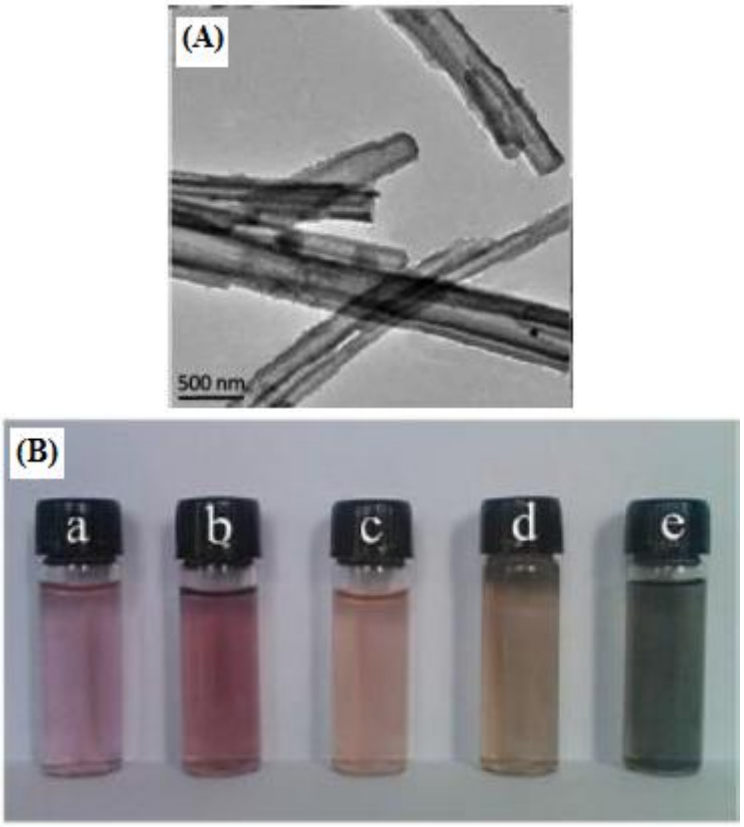

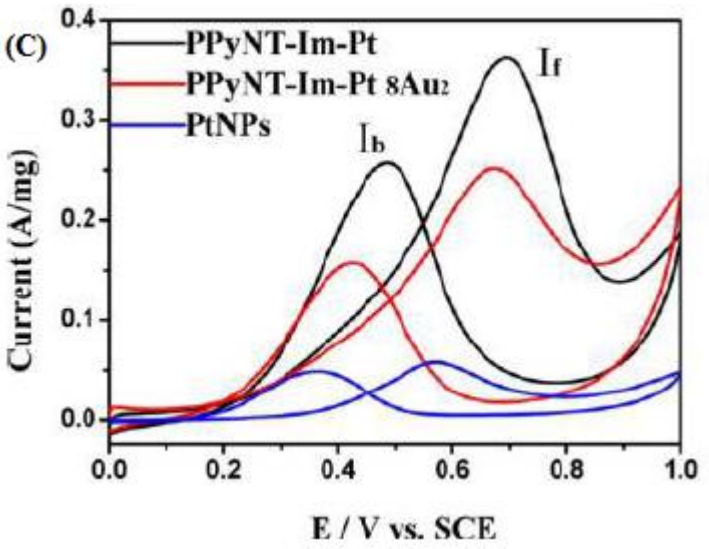

Figure 6. (A) TEM images of PPyNT-Im-Au hybrids (B) Photograph of colloidal aqueous solution containing 0.1 mM (a) PPyNT-Im-Au, (b) PPyNT-Im-Pt_2Au_8, (c) PPyNT-Im-Pt_5Au_5, (d) PPyNT-Im-Pt_8Au_2 and (e) PPyNT-Im-Pt hybrids (C) CVs (Scan rate: 50 mV s^{-1}) of PPyNT-Im-Pt, PPyNT-Im-Pt_8Au_2 and Pt NPs hybrids for methanol oxidation at 0.6 V (vs SCE). ("Reprinted with permission from (*ACS Appl. Matter. Interfaces* 5 (2013) 2752-2760). Copyright (2013) American Chemical Society").

The bimetallic electrode of Pt-M (M = Fe, Co and Ni) has been used as the chemical oxidation of carbon nanotube to form a new Pt-M/CNT composite. The study of electrocatalytic oxidation of methanol, cyclic voltammetry and chronoamperometry experiments showed highest electrocatalytic activity, CO tolerance and excellent stability for the positive development of DMFCs [63]. Recently, polypyrrole nanotube imidazolium moiety can be modified with Pt-Au alloy nanoparticles (PPyNT-Im-Pt_8Au_2) hybrid has been synthesized by covalently attached imidazolium moiety. By using TEM (Fig.6A) analysis, the morphological mean diameter value of ~13.2 nm and Fig.6 (B) shows the photograph of various dispersed aqueous solution containing different catalysts. The observed results were clearly indicated that, PPyNT-Im-Pt_8Au_2 hybrid exhibited well dispersed effect due to the mutual interaction between Au and Pt. Fig.6 (C) shows the well defined voltammogram peak current value of PPyNT-ImPt (0.36 A mg^{-1}) and PPyNT-Im-Pt_8Au_2 (0.25 A mg^{-1}) obtained higher current than that of PtNPs [64]. Giorgi *et al* [65] prepared an innovative platelet carbon based nanofiber and bimetallic of Pt-Au (PtAu/pCNF) nano catalyst by plasma enhanced chemical vapor deposition (PECVD) using methane and hydrogen as precursor. The matrix (PtAu/pCNF) was investigated the electrocatalytic oxidation of methanol. The one-step simple reduction rout to synthesize a bimetallic nanoparticles (Pt-Pd NPs) supported graphene (G) (Pt-Pd NPs/G) composite provided a novel superior electrocatalytic activity and good stability towards methanol oxidation reaction [66]. A rapid reducing method has also been used to prepare well aligned magnetic Pd-Co bimetallic nanoparticle supported on reducing graphene oxide sheets (Pd-Co/RGO). The electrode surface of TEM analysis, the mean average size of Pd-Co bimetallic nanoparticle was obtained about 10-13 nm [67]. Dong *et al* [68] have used a well distributed Pd/Cu bimetallic nanoparticles were deposited on graphene nano sheets (Pd/Cu/Graphene)

for direct ethanol fuel cell (DEFCs) applications. The hybrid of Pd/Cu/Graphene-3 catalysts exhibits optimal electrocatalytic activity and reached the highest electrocatalytic activity value I_f of 392.6 mA $mg^{-1}{}_{pd}$.

2.7. Metal oxides based catalysts

A graphite-based Pt supported electrode modified with In+Pb oxide has been obtained through the innovative electrochemical application of methanol oxidation reactions. The oxide based catalyst obtained very low oxidation potential (-30 mV), highest electrical conduction and sufficient electrode stability [69]. Huang *et al* [70] used a heterogeneous strong coupled with metal and metal oxide (Pt-SnO_2) can be modified with graphene oxide (Pt-SnO_2-prGO).

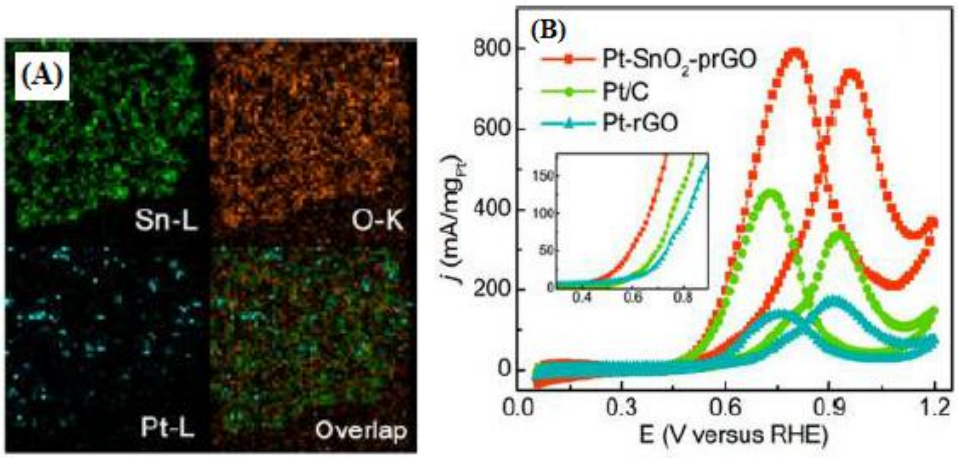

Figure 7. (A) HRTEM images of SnO_2-prGO (B) CV curves on Pt-SnO_2-prGO, Pt/C, and Pt-rGO in 2M CH_3OH + 0.1 M H_2SO_4 solution with a sweep rate of 50 mV s^{-1}. ("Reprinted with permission from (*ACS Appl. Mater. Interfaces* 6 (2014) 10258-10264). Copyright (2014) American Chemical Society").

The morphological (Fig.7 (A) STEM,) and unexpected higher methanol oxidation synergetic peak current density of Pt-SnO_2-prGO catalyst was 739.8 mA mg_{pt}^{-1} (Fig.7 (B)). The low temperature hydrothermal method has been used to create a platinum supported lanthanum-doped tantalum oxide (La-Ta_2O_5/Pt) irregular with aggregation nanoparticle. By using density functional theory (DFT) calculation, which can be estimated the improvement of electrical conductivity and electrocatalytic activity of Ta_2O_5 [71]. The electrochemical method using tantalum oxide-modified Pt based novel catalyst, opening up a new application for fuel cell studies in acidic medium. The modified electrode, concurrently with a favorable shift of the onset potential of methanol oxidation and the investigated apparent activation energy E_a value of 39 KJ mol^{-1} [72]. A simple washing and the ultrasonically treated rout was applied to prepare Pt/MWCNT and a nanocomposite of Pt supported manganese oxide with MWCNTs (Pt/MnO_x-MWCNTs). These catalysts were examined through cyclic voltammetry and linear sweep voltammetry. The exhibited methanol oxidation catalytic current enhancement value of 3.5 times higher for Pt/MWCNT and 4.6 times higher for Pt/MnO_x-MWCNTs. Similarly, the electrode

surface area value of 29.7 for Pt/MWCNT and 89.4 m^2 g^{-1}_{pt} for Pt/MnO_x-MWCNTs [73]. Huang *et al* [74] used a facile method to prepare the two-dimensional sandwich-like Pt/Mn_3O_4/reduced graphene oxide (RGO) nanocomposite for fuel cell applications. Zeng *et al* [75] investigated the methanol oxidation on an ordered mesoporous carbon doped electrode modified with tungsten hybrid (OMC-WO_3) composite which was prepared by template and thermal decomposition method.

2.8. Polymer electrolyte based fuel cell

The electrocatalytic effects of PtRu/C anode have been reported for mixed reduction of solid polymer-electrolyte direct methanol fuel cell (SPE-DMFCs) applications. The cathode of RuSe/C yielded the high performance and the achieved power density value of approximately 50 and 20 mW cm^{-2} [76]. The membrane scalable of $LaNiO_3$/CNT catalyst can be obtained by the sol-gel method using 60 wt % acetylene black, 40 wt % polytetrafluoro ethylene, 30 wt % of a noble metal (Ni) and 45 wt % of CNT were mixed in to slurry and then coated with uniformly. The membrane catalyst was annealed at 340º C for 1 hr and it can be used for DMFC can reach the power density value of 103 mW cm^{-2} [77]. The electrocatalytic active Pt(Cu)/C and Pt-Ru(Cu)/C catalysts have been prepared by potentiometric deposition and galvanostatic exchange method on Vulcan carbon XC72R. The catalysts have been explored higher activity and enhanced specific current for methanol oxidation [78]. Higa *et al* [79] used a block type of polymer electrolyte membrane (PEMs) were prepared by casting method of poly(vinyl alcohol-b-styrene sulfonic acid) and by cross-linking the PVA chains with glutaraldehyde (GA). The block type of PEMs was reported 32.4 mW cm^{-2} of P_{max} under 116 mA cm^{-2} of loaded current density. Another approach has been the proton exchange membrane (PEM) with an interpenetrating network of polyvinyl alcohol and poly(vinyl alcohol-co-2-methyl-1-propane sulfonic acid). By applying the PVA based PEM membrane delivered a maximum power intensity value of (P_{max}) 2.4 mW cm^{-2} using 2M methanol [80]. Katiyar *et al* [81] reported the comparative analysis of six multiple reactor R configurations, namely FBR_1 (Fixed bed reactor), MR_1 (H_2 selective membrane reactor with one reaction tube), MR_2 (H_2 selective membrane reactor with two reaction tube), FBR_2 (FBR_1 + Preferential CO oxidation (PROX reactor)) and MR_4 (MR_2 + PROX). In these membrane based reactors, MR4 generates compact and innovative fuel cell of methanol oxidation, which exhibited 470 W PEMFC.

2.9. Composite based catalyst

The preparation of Pt-Co bimetallic compounds were deposited on polypyrrole-multi-walled carbon nanotube composite by *in situ* polymerization method, for the investigation of its reduction rout to the development of an anode catalyst for direct methanol fuel cells (DMFCs). The composite reached good CO-tolerance ability and great potential for DMFCs [82]. Zhou *et al* [83] developed an electrocatalytic performance of methanol oxidation based on a novel modified composites of platinum supported poly indole (Pt/Pin/GC) and poly(5-methoxy indole) (Pt/PMI/GC) in a electro deposition method. The Pt/Pin/GC and Pt/PMI/GC catalysts were revealed higher catalytic activity and strong poisoning-tolerance. Electrochemical impedance spectroscopy also used to measure the charge-transfer

resistance for methanol oxidation. Methanol oxidation fuel cell based on Pt-Co supported polyphosphazene modified with carbon nanotube was reported [84]. The composite fuel cell showed good distribution, small particle size and high mass activity.

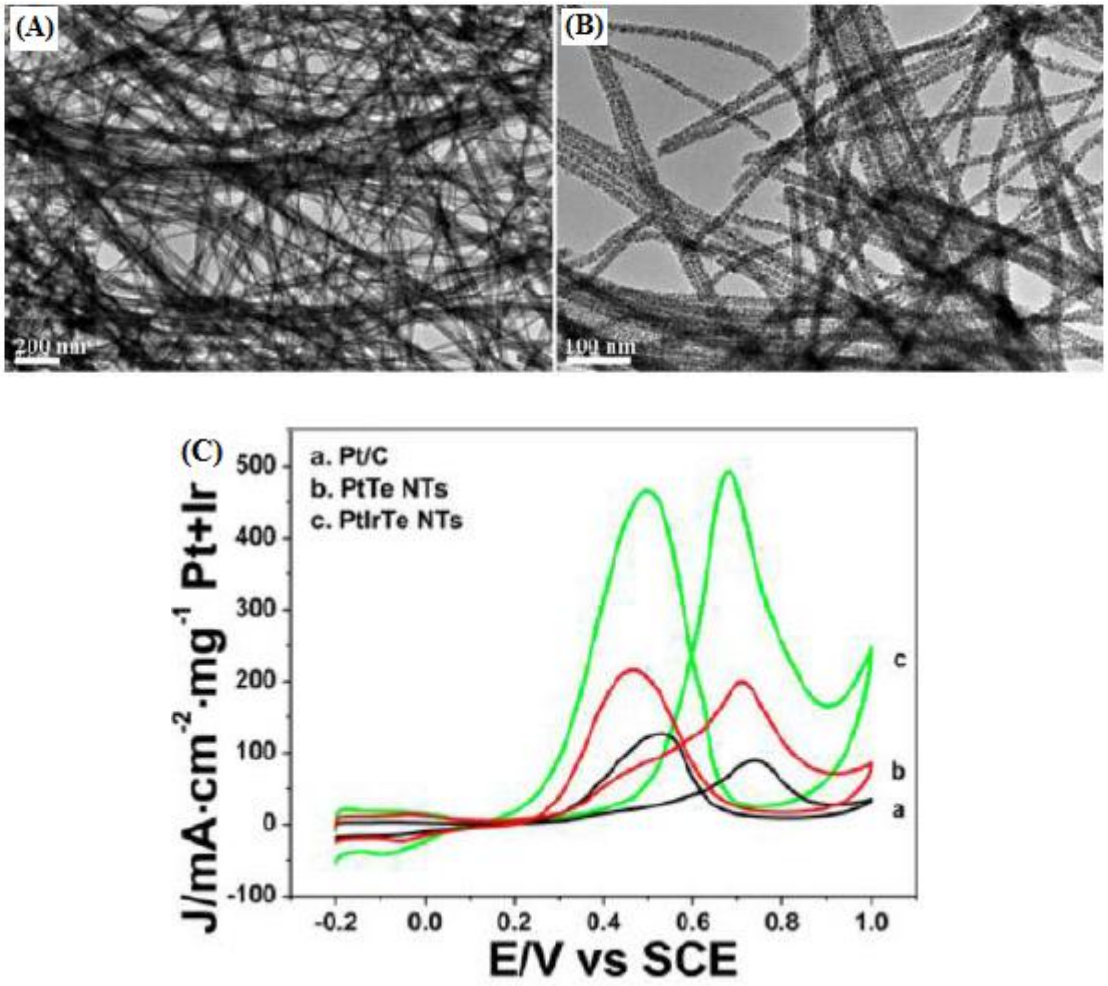

Figure 8. TEM images of PtIrTeNTs under different magnification (A) 200 nm, (B) 100 nm and (C) CV curves of PtIrTeNTs, PtTeNTs and Pt/C catalysts in 0.5M H_2SO_4+0.5M CH_3OH solution at the scan rate of 50 mV s^{-1}. ("Reprinted with permission from (*ACS Appl. Mater. Interfaces* 6 (2014) 21986-21994). Copyright (2014) American Chemical Society").

A bimetallic of PtAu nanoparticle supported on polydopamine and modified with reduced graphene oxide (PtAu/PDA-RGO) catalyst has been investigated for the active catalyst for methanol oxidation reaction. The PDA plays an important role in the enhancement of dispersion and the stability of electrocatalytic activity. Bimetallic catalyst of PtAu/PDA-RGO exhibit better catalytic activity than mono catalytic Pt catalyst [85]. A nickel based TiO_2 nanotube array (Ni/TiO_2 NTs) composite showed remarkable enhanced catalytic activity and excellent stability for methanol oxidation reaction under illuminated conditions [86]. Hao *et al* [87] was used a wet chemical method to developed ultra long PtIrTe nanotubes (NTs) (PtIrTeNTs). Fig.8 (A) & (B) shows the two different magnification TEM images of PtIrTeNTs, Pt component presented a nano dendrited array on the surface of IrTeNTs. In

Fig.8 (C) of PtIrTeNTs catalyst exhibited higher electrocatalytic activity (495 mA cm^{-2}) than other Pt/C catalyst.

3. EFFECT OF PARAMETERS

3.1. Annealing effects

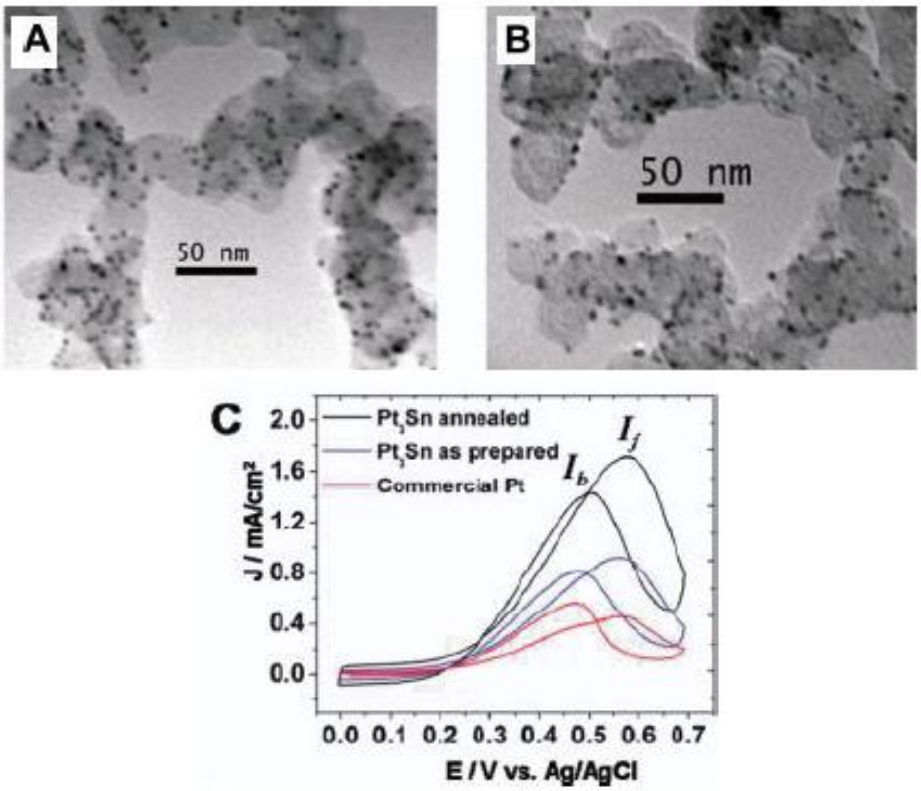

Figure 9. TEM images of (A) the Pt_3Sn as prepared and (B) the Pt_3Sn Annealed (under Ar + 5% H_2 at 400° C for 1 h) (C) CVs of J-V curves reflecting MOR catalysis in 0.1 M $HClO_4$ and 0.1 M methanol with a potential sweeping rate at 50 mV/s. ("Reprinted with permission from (*ACS Catal.* 1 (2011) 1719-1723). Copyright (2011) American Chemical Society").

The enhanced electrocatalytic activities bimetallic nanowires of Pt_3Co catalyst has been prepared by template-assisted pulsed electro deposition method. The catalysts were annealed at different thermal treatments such as 200, 400 and 600° C, moreover the exhibited better electrocatalytic activities and magnetic properties were occurring at 200° C [88]. Another study by Prabhuram et al [89] made a membrane electrode assembly (MEA) by decade method for direct methanol fuel cell applications using commercial hydrocarbon membrane and nafion isomer. The catalyst was observed that decreased the stability only by 34 % degradation at the end of 500 Hrs. Recent literature demonstrated that, a core-shell structure of Bucky diamond (BD) has been prepared by annealing detonation-synthesis nano sized diamond in 10^{-3} pa vacuum at 900 - 1100° C. Microwave-assisted reduction method, which can be used to prepared a Pt supported BD and ND catalyst. The electro oxidation of methanol exhibits higher catalytic activity and higher stability for

Pt/BD than Pt/ND [90]. A chemical method to form a mono dispersed Pt_3SnNPs catalyst was subjected to methanol oxidation reaction. The TEM images showed (Fig.9. (A) & (B)) as-prepared Pt_3SnNPs & annealed (180° C - 240° C) Pt_3SnNPs. The annealed catalyst exhibited higher catalytic activity for methanol oxidation reaction as shown in Fig.9 (C) [91]. Simple hydrothermal and thermal solid state methods also led to the formation of two types of nitrogen-doped graphene catalysts. In this electrode catalysts were discussed few electrochemical and fuel cell parameters like, current density, power density, Tafel slope and resistance etc. In these electrode catalysts, Pt/NG180 + MWCNT exhibits maximum current density (1.20 A cm^{-2}) and the reported power density value of 704 mW cm^{-2} [92]. The thermal decomposition method was employed to obtain a Pt based ruthenium oxide ($Pt_xRu_{(1-x)}O_y$), which can be evaluated towards the methanol oxidation reaction. Notably, the electrode annealed at 400° C reported better structural and chemical properties favored during the calcinations processes [93].

3.2. Effect of morphology

A three-dimensional multi-component nano porous platinum-ruthenium-copper-osmium-iridium (np-PtRuCuOsIr) catalyst has been fabricated by chemically de-alloying of a mechanically alloy of AlCuPtRuOsIr precursor. The fabricated np-PtRuCuOsIr catalyst exhibit higher mass activity value of 857.5 mA mg^{-1}_{pt} and the specific activity value of 3.0 mA cm^{-2} for methanol oxidation. The bi-continuous ligament/channel structure with an average diameter value of ~2.5 nm and it can act as excellent catalytic activity as well as CO tolerance towards methanol oxidation reaction [94]. Wu *et al* [95] reported the nano structured of poly(aniline-co-metanilic acid) catalyst prepared by chemical oxidative polymerization of aniline (Ani) and metalinic acid (Maa) (Ani/Maa). The Ani/Maa catalysts have been optimized with various molar ratios such as 40/1, 20/1, 10/1, 4/1, 2/1 and 1/1 respectively. From the TEM images were clearly indicated, the black spots of Pt nano particles. Specifically, P(A10-M)-Pt electrode surface is clearly reported the smaller particle size range of 10-20 nm than the other electrodes and it can be (uniform distribution and special neutral structure) expected to be very promising for methanol oxidation. Recently, platinum supported graphene oxide (GO) (Pt/GO) catalyst has been reported in the literature. The surface morphology of the layered structure of GO sheets and the agglomerated Pt nano particles were dispersed on the GO surface. The smaller particle size value around 2-3 nm and the catalyst exhibit better catalytic activity and higher reactivity [96]. The multi-component nano porous PtPdAlCu(np-PtPdAlCu) quaternary alloy electrode has been prepared by ball-milling with the subsequent-two step de-alloying processes. The catalyst exploited as an electrode in methanol oxidation. The contrast nano porous np-PtPdAlCu alloy was studied elemental analysis by using STEM and EDX mapping analysis. On the other hand, the voltammetry mass normalized current density of np-PtPdAlCu catalyst methanol oxidation reaction highest exhibited electrocatalytic activity of 360.8 mA mg^{-1}_{pt} than Pt/C (183 mA mg^{-1}_{pt}) [97]. Gharibi *et al* [98] studied a platinum supported polyaniline was electro polymerized from the aniline monomer and it was further electro reduced onto the carbon paper (Pt-PANI/Carbon paper) catalyst used for DMFC. The surface morphology of PANI appears highly porous to increase the PANI thickness and decreased the Pt particle size about 4 nm.

The surface roughed Pt nano wires have been evaluated by Ruan and his co-workers and reported that the methanol oxidation of surface roughed Pt catalyst better catalytic activity value of 109.5 mA mg^{-1}_{pt} and it can be contribute the improvement of catalytic performance [99].

3.3. BET surface

A nano structured carbon supported Cu@Pt-Pd core-shell electrode was evaluated the maximum electrochemical surface area (ESCA) value of 136 m^2 g^{-1}. In this type of galvanic deposited nanostructure of Cu@Pt-Pd catalyst applied the electrocatalytic activity for methanol and ethanol oxidation reaction [100]. The meso porous nanostructure of sodium dodecyl sulfate (SDS)-assisted nickel cobaltite ($NiCo_2O_4$) catalyst has been prepared by a facile hydrothermal method. $NiCo_2O_4$ exhibit a typical nano scale crystalline hexagonal morphology and its specific surface area (SSA) and mesopore volume estimated of 88.63 m^2 g^{-1} and 0.298 cm^3 g^{-1}. Notably, SDS-assisted $NiCo_2O_4$ electrode showed better electro oxidation (CH_3OH) and large surface intensities between Co and Ni [101]. The other interesting unprotected PtRu based nitrogen-doped carbon nano horns (PtRu/NCNHs) exhibits obvious enhancement of methanol oxidation reaction (MOR). The MOR of electrode mass activity value of PtRu/NCNHs at 850 mA mg^{-1}_{PtRu} than that of PtRu/C-JM (341 mA mg^{-1}_{PtRu}) [102]. Zhang *et al* [103] used PtRu nanoparticle supported nitrogen-doped mesoporous carbon (NMPCs) and the structural characteristics of ultra high NMPCs BET surface area value of 1960 m^2 g^{-1} and its pore volume of about 1.16 cm^3 g^{-1}. By using the prepared PtRu/NMPCs catalyst displayed much higher catalytic activity and good stability for methanol oxidation. A Pt-decorated 3D architecture built from graphene and g-C_3N_4 (Pt/G-CN) nanosheet array as-prepared by sonication suspension method displayed anode electro catalyst for methanol oxidation. The electro activity of Pt/G-CN architecture has been investigated by cyclic voltammetry method. Pt/G-CN architecture was identified their electrochemical active surface area (ESCA) of 69.0 m^2 g^{-1} by Columbic charge hydrogen adsorption method [104].

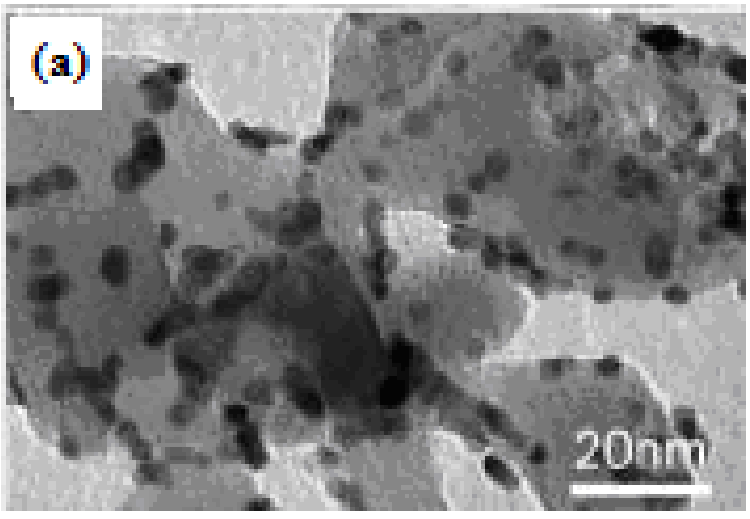

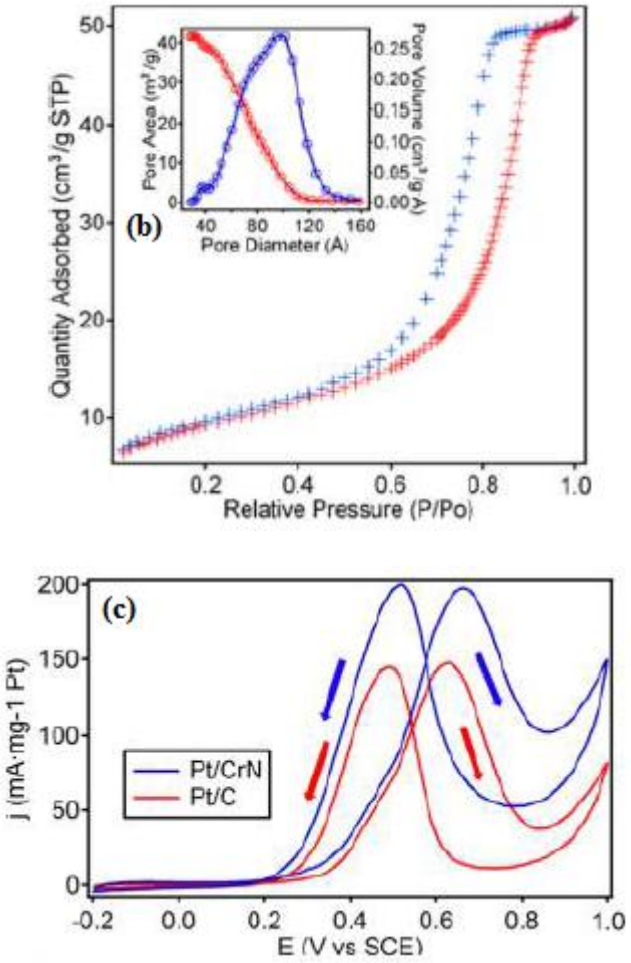

Figure 10. (a) TEM of the Pt/CrN catalyst (b) BET surface area of mesoporous CrN prepared by ammonolysis of $K_2Cr_2O_7$ at 700° C for 8 h (c) Cyclic voltammograms of Pt/CrN catalyst as compared to Pt/C catalyst in 0.6 V in 1 M CH_3OH + 0.5 M H_2SO_4 Solution. ("Reprinted with permission from (*Chem. Mater*. 25 (2013) 1783-1787). Copyright (2013) American Chemical Society").

The two distinct graphene sheets (wavy graphene and vacuum-promoted graphene) where the growth of platinum nanoparticles and they (w-GN/Pt & VPG/Pt) have been widely used as electrodes in methanol oxidation. Recently, studies have shown that the average size of Pt Nps on the wavy graphene sheets around 2 nm and the BET analysis showed the specific surface area (SSA) value of VPG 356 and w-GN for 431 m^2 g^{-1} respectively [105]. Yang *et al* [106] demonstrated novel kinds of platinum supported meso porous chromium nitride (Pt/CrN) and Pt/C for electrochemical applications. These types of electro catalysts were optimized the electrochemical active specific surface area (ESCA) value (Fig.10.b) of 82 and 75 m^2 g^{-1}. In Fig.10.a, the TEM image of the CrN pores on the scale of 5-10 nm. On the other hand voltammetric analysis (Fig.10.c), showed greater catalytic activity for methanol oxidation.

4. TECHNIQUES FOR MOR

4.1. Cyclic voltammetry

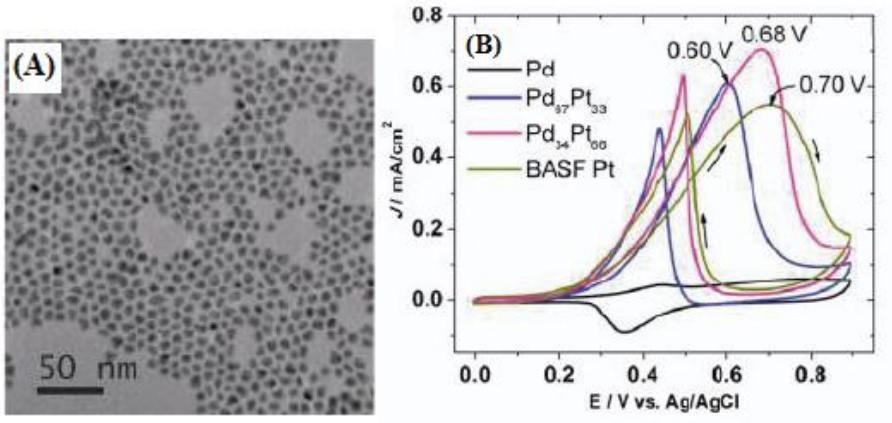

Figure 11. (A) TEM images of 6.5 nm $Pd_{67}Pt_{31}$ NPs (B) J-V curves reflecting MOR catalysis of NP catalysts in 0.1 M $HClO_4$ and 0.1 M methanol. ("Reprinted with permission from (*Chem. Mater*. 23 (2011) 4199-4203). Copyright (2011) American Chemical Society").

A facile synthesis of polyhedral PdPt alloy nanoparticle has been synthesized from morpholine borane reduction of $Pd(acac)_2$ and $Pt(acac)_2$ in oleyamine. Fig.11. (A) & (B) TEM image shows the typical mono dispersed a uniform surface catalyst used in the electrocatalytic oxidation of methanol [107]. Polyaniline (PANI) modified with para toluene sulfonic acid (PTSA) by doping-de-doping-re-doping resulted in PANI-PTSA composite, further it can be modified with Pt on the electrode surface (Pt/PANI-PTSA). The catalyst was characterized by electrochemically and it (Pt/PANI-PTSA) was used for methanol oxidation at the Pt electrode surface in 1M CH_3OH [108]. Miao and Tao [109] performed on the silicone micro channel plates (MCP) modified with nickel, palladium (Ni-Pd) nano particles by the electroless plating method. The catalyst of Ni-Pd/Si-MCP showed a remarkable electrocatalytic activity towards the methanol and ethanol oxidation by using cyclic voltammetry and chrono potentiometry in alkaline medium. A three-dimensional electrode Pt on a polypyrrole treated polystyrene sphere (Pt/Ppy/PS) catalyst, making a profound impact in electrochemistry due to its remarkable electrochemical properties of methanol oxidation. The sphere type of Pt/Ppy/PS electrode catalysts exhibit particle size range around 200 nm – 2μm and it could be big and small holes like structure. The authors have optimized different kinds of catalysts electrochemical surface area behaviors like Pt/Ppy/200nmPS, Pt/Ppy/450nmPS, Pt/Ppy/200nm-2μmPS and E-Tek Pt/C electrodes were found to be 33.5, 67.5, 72.5 and 32.5 m^2 g^{-1} respectively [110]. Cooper *et al* [111] used the ternary alloy systems of Pt-Ru-W and Pt-Ru-Co were examined for used as anode catalyst in DMFCs. The identified results were clearly indicated that the composition as being active for methanol oxidation in the short term may act under longer steady state conditions. This is due to explained that high surface area powders in a more efficient catalyst in fuel cell atmosphere. The membrane electrode assembly (MEA) has been prepared by "two-step conditions method" for power-generation improvement of DMFCs. Thus the optimized conditions containing terms 9 to 10 Hrs, H_2 containing

temperatures 80º C, the significant improvement of maximum power density values are 69.4 mW cm^{-2} for 1 mol dm^{-3}, 48.8 mW cm^{-2} for 5 mol dm^{-3}, 32.2 mW cm^{-2} for 10 mol dm^{-3} [112].

4.2. Electrochemical impedance spectroscopy (EIS)

Platinum supported carbon based catalyst was modified with metal oxides (CeO_2, TiO_2 and SnO_2), they can easily act as enhancing agent for efficient acceleration of electron transfer between electrode and the detection molecules, leading to more rapid electro oxidation of methanol (0.5M CH_3OH) by EIS analysis [113].

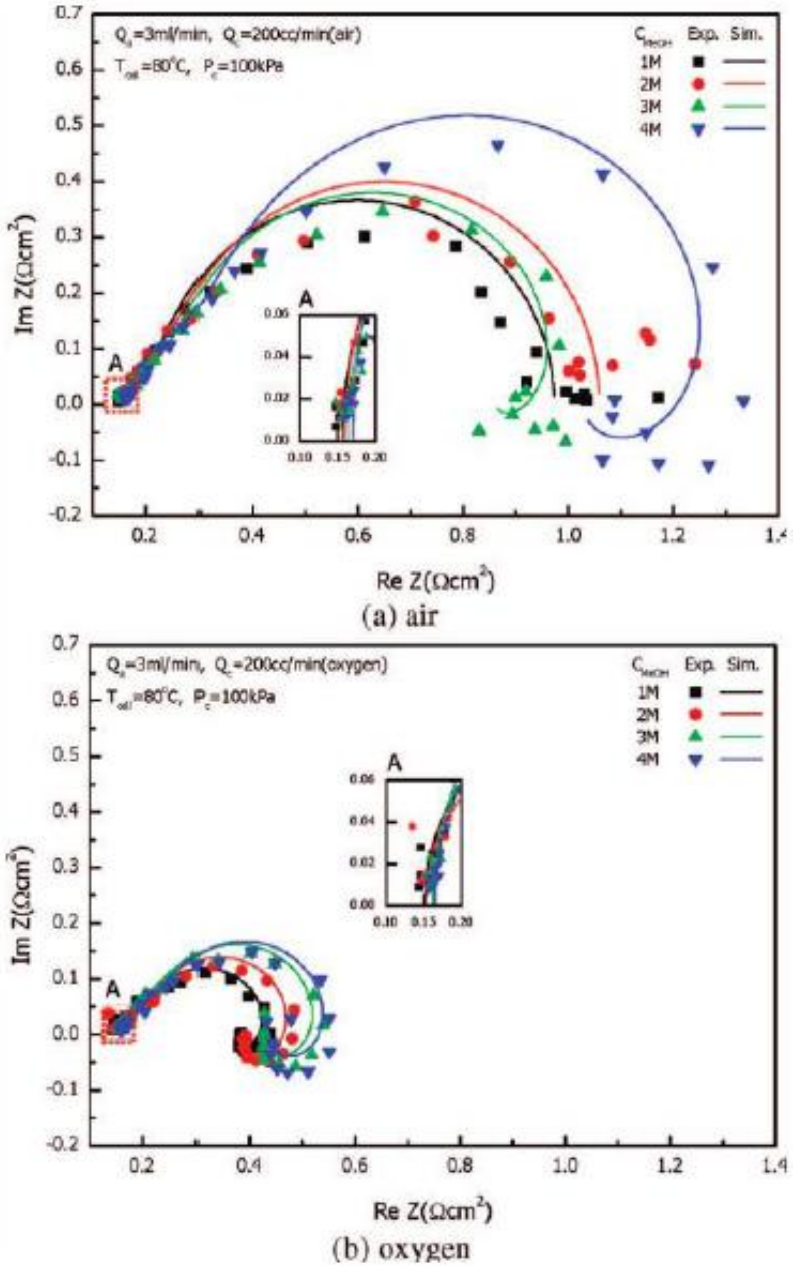

Figure 12. Effect of MeOH concentration on the DMFC Nyquist diagram. ("Reprinted with permission from (*Energy & Fuels* 22 (2008) 1204-1211). Copyright (2008) American Chemical Society").

The gas diffusion electrode is another attractive modified surface carbon (Ketjen black) supported Pt_3Co catalysts were used methanol fuel cell applications. The electrochemical parameters of charge-transfer resistance (R_{CT}), double-layer capacitance, relaxation resistance and relaxation induction have been evaluated by EIS. The catalytic activity of Pt_3Co/KB reported a remarkable power density value of 31 mW cm^{-2} [114]. A nano particulate PtRu fuel cell anode of a commercially available membrane electrode assembly (MEA) displays fascinating electrocatalytic properties for the mechanistic investigation of methanol oxidation by EIS. Particularly, before the onset potential gradually increasing the R_{CT} values with potential attributed to the blocking of active surface area. On the other hand, the gradual decreases of R_{CT} value with increasing after the onset potential values [115]. Electroctalytic oxidation of methanol was investigated by two different electrodes such as the Pt-Ru-Ni/C and Pt-Ru/C. By these analyses, they have discussed three different rates-determining step of oxidations like dehydrogenation, oxidation reaction adsorbed CO_{ads} and OH_{ads} in the low potential region (400-500 mV) and high (600-800 mV) potential for oxygen evolution. The higher electrocatalytic methanol oxidations were reported at Pt-Ru-Ni/C catalyst than that of Pt-Ru/C [116]. Seo *et al* [117] investigated the electrochemical impedance study of DMFCs operated under various conditions such as temperature, methanol flow rate, methanol concentrations, cathode flow rate and type of oxidant gas. All the above parameters only a maximum performance of DMFC was achieved by the reduced impedance at a methanol concentration of 1M with oxygen as the oxidant gas as shown in Fig.12. Chen et al [118] developed a novel mathematical stimulated model by using EIS for the cathode of DMFCs. In this EIS pattern was strongly dependent on the applied electrode potential, which can be used to optimize the R_{CT} value and CO adsorption relaxation.

4.3. Tafel slope

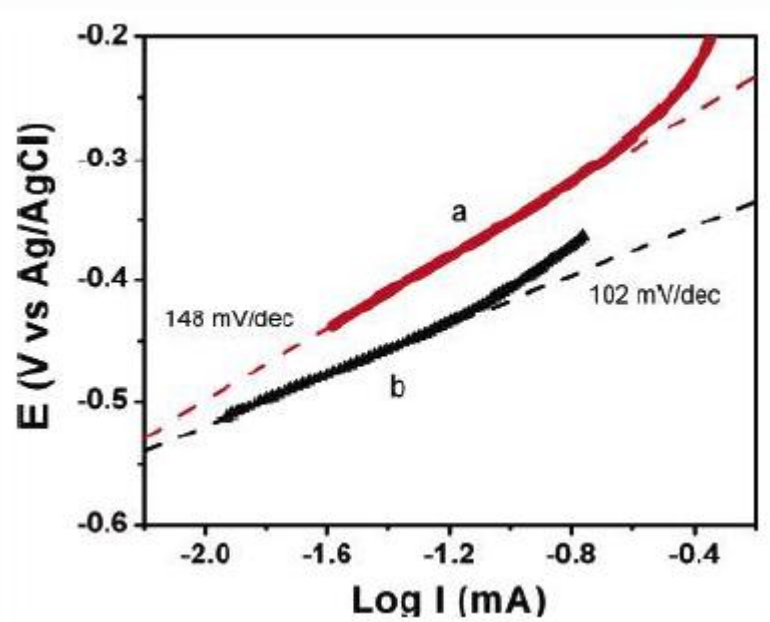

Figure 13. Tafel plots for $Au_{82}Pt_{18}$/C (a) (treated at 500° C) and PtRu/C (b) catalysts (on GC electrode, 0.07 cm^2) in 0.5M KOH with 0.5 M methanol. ("Reprinted with permission from (*Langmuir* 22 (2006) 2892-2898). Copyright (2006) American Chemical Society").

Girishkumar *et al* [119] used in varying amounts of thin film based single-walled carbon nano tube (SWCNT) by electrophoretic deposition method for methanol oxidation. The two-distinct Tafel slopes were discussed into two regions, one exhibit lower current region and other obtained higher current at CNT/Pt electrode. From the slope, the onset potential of methanol oxidation suggests that the CNTs have a major catalytic effect on the electrode surface reaction. The as-prepared nano clusters of Pt_3RhNC wrapped by a formic acid reduction in the development of potential electrocatalytic oxidation of methanol. The catalyst showed a mass activity value of 1392.5 ma mg^{-1} and the current (I_f/I_b) ratio nearly 3-fold higher than that of Pt_3RhNC/VC. By using Tafel slope, the electrochemical investigation has been estimated for the possible mechanistic pathway [120]. Based on a novel carbon supported bimetallic AuPt nanoparticle (AuPt/C) has been investigated the electrocatalytic methanol oxidation reaction (MOR). The comparative study of the Tafel curve (Fig.13), $Au_{82}Pt_{18}/C$ (Annealed at 500º C) and PtRu/C catalyst in 0.5M methanol under alkaline conditions. Here $Au_{82}Pt_{18}/C$ catalysts exhibit 148 mV/dec, which was greater than that of PtRu/C [121]. In another study, cyclic voltammetry and rotating disc electrode (RDE) techniques were developed based on carbon-supported Pt-Ru electrode catalyst for the evaluation of methanol oxidation. The fuel cell showed oxidation irreversible behavior of an exchange current density of 2.3 x 10^{-6} A cm^{-2} and Tafel slope value of 113 mV dec^{-1}. The possible proposed methanol oxidation sequence on Pt-Ru catalyst in a fuel cell configuration can be strongly affected by the mass-transport conditions [122]. Gonzalez *et al* [123] developed a micro-wave assisted chemical reduction method was fabricated $PtSnO_2/C$ catalyst as an anodic active material for DMFCs. Tafel study has been used for the investigation of some kinetic parameters like charge-transfer coefficient and electrode catalytic performance. The electrode catalyst was reported to be stable up to 150 cycles. The electro oxidation and mass corrected slopes were applied for the studies of methanol oxidation with the catalytic performance of carbon supported PtRuMo/C catalyst showed the highest tolerance to methanol intermediates and the founded Tafel slope values 0.060 V $decade^{-1}$ [124].

4.4. Polarization curve

Chen *et al* [125] have used blended learning fitting algorithm (BLFA) method of polarization curves for fuel cell applications. The algorithm, simulated with MATLAB environment, which was less than 0.15% time consuming of classical non-linear least square estimation. The algorithm model exhibits accurately fitted with an average quadratic error of 0.6% E_{OC} for PEMFC and 1.14% for DMFC. Bruno *et al* [126] investigated PtRu nanoparticle supported on a mesoporous carbon (MC) (PtRu/MC) anode catalyst for electrocatalytic applications. In Fig.1shows the polarization and power intensity curves were explained that a better electrochemical performance of PtRu/MC catalyst at 30° C and 60° C, the yielded power intensity values of 40 and 67 mW cm^{-2}. Moreover, the methanol oxidation exhibited higher current densities and reduced the over potential values. Kang *et al* [127] established the shape controlled synthesis of cubic and spherical bimetallic nanocrystals of Pt-ZnNCs. This electrode catalyst was highly active towards methanol oxidation with spherical shape catalyst exhibited higher activity than cubic NCs as shown in Fig.14. Poly(vinyl alcohol)/sulphated *β*-

cyclodextrin composite catalyst has been prepared by the proton exchange method for DMFCs applications.

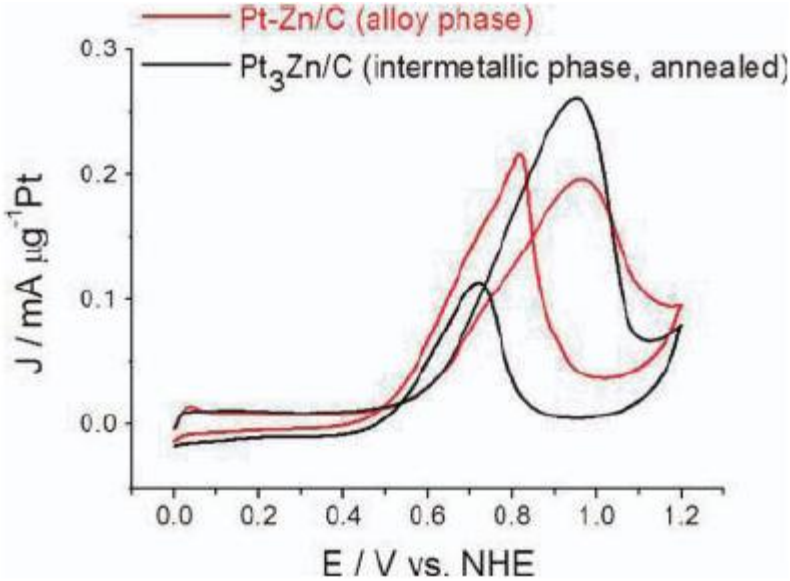

Figure 14. Polarization curves of methanol oxidation on alloy phase Pt-Zn/C and intermetallic phase Pt_3Zn/C catalysts. ("Reprinted with permission from (*ACS Nano* 6 (2012) 5642-5647). Copyright (2012) American Chemical Society").

However the proton conductivity and methanol permeability were exhibited in high reducing at 353K and 2M methanol [128]. The corrosive resistance performance of $SS_{31}6L$ (Stainless steel electrode) catalyst has been tested by electrochemical impedance spectroscopy (EIS), the test showed the polarization resistance value of untreated and treated SS316L were obtained 1191 Ω cm^2 and 9335 Ω cm^2 respectively. By using $SS_{31}6L$ catalyst, the electrocatalytic oxidation of methanol was achieved the power intensity value of 1.18 mW cm^{-2} at ambient condition [129]. Platinum and Pt-Ru supported multi-walled carbon nanotubes (Pt/MWNT and Pt-Ru/MWNT) have been synthesized by CVD and chemical reduction methods using AB_3 alloy hydride catalysts. The high performance of DMFC has been used the electrode catalyst of Pt-Ru/MWNT, the reported maximum power density value of 39.3 mW cm^{-2} at a current density of 130 mA cm^{-2} [130].

4.5. Electrode performance

A significant study of hydrous ruthenium oxide ($RuO_2.xH_2O$) catalyst provides the dynamic response and quasi-steady state performance of the DMFC. There has been only one report on the cell with $RuO_2.xH_2O$ layer (ROL) sandwiched between anode catalyst and gas diffusion layer, the reported power density value of 87 mW cm^{-2} which was 16% higher than that of conventional one [131]. A detailed study of the electrochemical switching of high performance membrane electrode assemblies (MEAs) and its electrocatalytic and morphological properties has been reported. The study revealed that the EIS and polarization curve analysis showed an increasing of thickness properties and the porosity of cathode electrode play an important role to improve their cell performance and reduced the

cathode reaction resistance [132]. The TEM morphological and the different annealed temperature polarization studies of PtRuMo/CNTs have been explored in detail by Chen *et al* [133]. The optimized morphological structure of PtRuMo nano particles average diameter range of 2-4 nm and were uniformly distributed on the CNT electrode surface. Meanwhile, the polarization analysis was evaluated at three different annealed temperatures such as 25, 40 and 60° C yielded their respective power intensity values like 23.54, 38.24 and 61.32 mW cm^{-2}. Prakash *et al* [134] studied the effect of electrode surface of methanol oxidation on alkaline anion exchange membrane (AAEM). They investigated; AAEM and noble metal electrode catalyst achieved their power density values between 25 and 168 mW cm^{-2} depending on their operating conditions, such as temperature, fuel composition and used electrode materials. A sulfonated graphene oxide (SGO)/nafion composite membrane modified electrode has been investigated for DMFCs applications. The SGO/nafion composite membrane exhibits 20° C higher tan δ values than pristine sample; this is due to contribute a large interface between exfoliated SGO and nafion catalysts and also the performance curve exhibited a maximum power intensity value of 49.9 mW cm^{-2} at 102.7 mA cm^{-2} [135]. Araya *et al* [136] employed the high performance of a high temperature proton-exchange membrane fuel cell (HT-PEMFC) studies at various temperatures (140° C to 180° C). The applied H_3PO_4-doped poly benzimidazole (PBI) based membrane electrode assembly (MEA) estimated the electrode active surface area value of 45 cm^2. By using EIS analysis, the estimated conductivity and electrode activity slightly reduced and the overall endurance test of performance for 100h at 90% conversion.

4.6. Power density

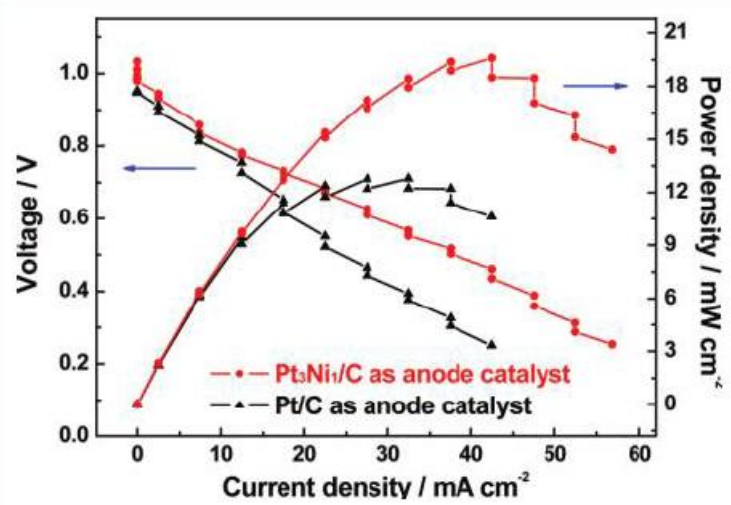

Figure 15. Single-cell tests performed with the Pt/C and the Pt_3Ni_1/C as the anode catalyst, respectively. The metal loading for the anode is 2 mg cm^{-2}. The cathode catalyst is 40 wt % Pt/C (Johnson Matthey), Inc.; the Pt loading is 1 mg cm^{-2}. The anode feed is 1 M NaOH + 1M CH_3OH with a flow rate of 1 mL min^{-1}; the cathode feed is O_2 under the pressure of 0.2 MPa. ("Reprinted with permission from (*J. Phys. Chem. C* 114 (2010) 19714-19722). Copyright (2010) American Chemical Society").

Jiang *et al* [137] reported that a carbon-supported bimetallic Pt_mNi_n (PtNi/C) catalyst has been synthesized by polyol process. The superior electrocatalytic activity towards methanol oxidation reaction has been optimized in alkaline conditions. The applied high open circuit voltage (OCV) acted as faster kinetic reaction in both MOR and ORR under alkaline conditions. The Pt_3Ni_1/C catalyst reported maximum power density value of 19 mW cm^{-2} than Pt/C (13 mW cm^{-2}) as shown in Fig.15. The application of novel toray carbon paper (TCP) self-assembled and also carbon paper (CP) self-assembled monolayer of MWCNT in combination with nafion (N_f) coated osmium tetroxide (Os) laccase (TCP/CP-MWCNT-N_f-Os-laccase) composite catalyst has been reported for the generation of bio-fuel cell from the methanol oxidation reaction. The globular mass distributed well over the hydrophilic layer of bio-cathode materials are highly efficient with a maximum power density value of 46 □W cm^{-2} at an optimum condition of 1M methanol [138]. A triple-layer proton exchange membrane modified chitosan biopolymer electrode has been tested for high performance direct methanol fuel cell applications (HPDMFCs). The impregnated catalyst was reported the increasing of power output 68 mW cm^{-2} and also it could be conditioned as an easy preparation, low cost and promising electrode materials for HPDMFCs applications [139]. A more sophisticated approach an efficient electrocatalytic oxidation of methanol and formic acid by using porous platinum nano chains (Pt NCs) and platinum nano flowers (Pt NFs). The TEM images of 3D nano structured Pt NFs, the average surface dimension of the particle to be 10-20 nm, whereas the nano chain like morphology were obtained uncontrolled haphazard arrangement to be 8-12 nm. These different morphological catalysts have been investigated in the electrochemical studies of methanol oxidation [140]. Arikan *et al* [141] synthesized nano structured binary and ternary alloys (Pt-Pd and Pt-Pd-Ru) on Vulcan XC72-R by polyol and co-deposition method. The ternary Pt-Pd-Ru/C nano catalyst showed higher power density values of ~120 mW cm^{-2} than that of Pt/C at 90° C as shown in Fig.1. Electrocatalytic effects of PtRu deposited on Vulcan XC-72 carbon and a high surface area of IrO_2 support have been reported [142]. PtRu nanoparticle of 1.6 nm has been deposited on over Vulcan carbon and a lattice of IrO_2 by sulfite complex method. Between PtRu/C and IrO_2 matrixes exhibited better electrocatalytic activity (31 mW cm^{-2}) of methanol oxidation at 90° C. The electrocatalytic study of thinning anode gas diffusion layer (GDL) has been used for the cell performance study of DMFC exhibits the optimized temperature (60° C) reached 69.5 mW cm^{-2} [143]. Incipient wetness and ball milling methods were used to prepare Ni-modified $La_{0.6}Sr_{0.4}Fe_{0.8}Co_{0.2}O_3$-$Ce_{0.9}Gd_{0.1}O_2$ composite for the investigation of DMFCs in solid state fuel cell (SOFCs) applications. In this catalyst plays an important role in electrocatalytic activities, which was the reported power density value of about 350 mW cm^{-2} [144].

5. CONCLUSION

In summary, the electrocatalytic properties of different electrode materials have been discussed by monitoring their preparation, electrode surface area roughness and the power conversion efficiency values. Mainly, the electrocatalytic stripping of CO and methanol oxidation has been observed. Recently, many of the researchers were focused on commercially available cost-effective materials, simple fabrication method, superior electrocatalytic properties and long-term durability of

electrochemical reactions. From the rapid progress and vast development, DMFCs act as promising alternative energy conversion technology for the energy requirement of stationary power supplies (Inverters and UPS) and transportations (Cars and bikes). DMFCs, undoubtedly will contribute the future energy technologies, great effort for the large-scale productions on quality controlled low pollutant emission and high-energy power conversion efficiencies. Finally in this article, we have highlighted all kinds of electrode fabrication methods and discussed the exhibited lower level to maximum obtained power densities values methanol oxidation reaction.

ACKNOWLEDGEMENT
The authors would like to thank Dr. A. Xavier, Associate Professor & Head, Department of Chemistry, The Madura College, Madurai, Tamil Nadu and Natarajan Biruntha Devi, Graduate student, S.V.N College, Madurai, Tamil Nadu, India for their valuable suggestion on the fuel cell analysis.

References

1. M. Uchida, Y. Aoyama, N. Eda, A. Ohta, *J. Electrochem. Soc.* 142 (1995) 4143-4149.
2. E. Lee, A. Murthy, A. Manthiram, *J. Electroanal. Chem.* 659 (2011) 168-175.
3. S.F. Baxter, U.S. Battaglia, R.E. White, *J. Electrochem. Soc.* 146 (1999) 437-447.
4. Z. Jiang, J. Zhang, L. Dong, J. Zhuang, *J. Electroanal. Chem.* 469 (1999) 1-10.
5. S. Yu, Q. Liu, W. Yang, K. Han, Z. Wang, H. Zhu, *Electrochim. Acta* 94 (2013) 245-251.
6. R.E.Cid, P.H. Fernandez, J.C.P. Flores, S. Rojas, S.G. Rodriquez, E. Fatas, P. Ocan, *Int. J. Hydrogen Energy* 37 (2012) 7119-7130.
7. W. Ye, H. Kou, Q. Liu, J. Yan, F. Zhou, C. Wang, *Int. J. Hydrogen Energy* 37 (2012) 4088-4097.
8. H. Wang, R. Wang, H. Li, Q. Wang, K. Kang, Z. Lei, *Int. J. Hydrogen Energy* 36 (2011) 839-848.
9. A.S. Aarino, M. Borghei, I.V. Anoshkin, A.G. Nasibulin, E.I. Kauppinen, V. Ruiz, T. Kallio, *Int. J. Hydrogen Energy* 37 (2012) 3415-3424.
10. P.V. Samant, J.B. Fernandes, *J. Power Sources* 125 (2004) 172-177.
11. S. Wasmus, A. Kuver, *J. Electroanal. Chem.* 461 (1999) 14-31.
12. W. Yuan, B. Zhou, J. Deng, Y. Tang, Z. Zhang, Z. Li, *Int. J. Hydrogen Energy* 39 (2014) 6689-6701.
13. F. Lufrano, V. Baglio, P. Staiti, V. Antonucci, A.S. Arico, *J. Power Sources* 243 (2013) 519-534.
14. H. Bahrami, A. Faghri, *J. Power Sources* 230 (2013) 303-320.
15. S. Basri, S.K. Kamarudin, *Int. J. Hydrogen Energy* 36 (2011) 6219-6236.
16. J.H. Bang, *Electrochim. Acta* 56 (2011) 8674-8679.
17. D.J. Guo, J.M. You, *J. Power Sources* 198 (2012) 127-131.
18. B. Abida, L. Chirchi, S. Baranton, T.W. Napporn, C. Morais, J.M. Leger, A. Ghorbel, *J. Power Sources* 241 (2013) 429-439.
19. R. Shokrani, M. Haghighi, N. Jodeirim H. Ajamein, M. Abdollahifar, *Int. J. Hydrogen Energy* 39 (2014) 13141-13155.
20. S.M. Chen, R. Ramachandran, V. Mani, R. Saraswathi, *Int. J. Electrochem. Sci.* 9 (2014) 4072-4085.
21. R. Ramachandran, V. Mani, S.M. Chen, R. Saraswathi, B.S. Lou, *Int. J. Electrochem. Sci.* 8 (2013) 11680-11694.
22. R. Ramachandran, V. Mani, S.M. Chen, G.P. Gnanakumar, P. Gajendran, N. Birunthadevi, R. Devasenathipathy, *Int. J. Electrochem. Sci.*10 (2015) 3301-3318.

23. R. Ramachandran, V. Mani, S.M. Chen, G.P. Gnanakumar, M. Govindasamy, *Int. J. Electrochem. Sci*.10 (2015) 859-869.
24. K.J. Babu, A. Zahoor, K.S. Nahm, R. Ramachandran, M.A. Jothirajan, G. Gnanakumar, *J. Nanopart. Res*., 16 (2014) 2250.
25. V. Mani, R. Devasenathipathy, S.M. Chen, K. Kohilarani, R. Ramachandran, *Int. J. Electrochem. Sci*.10 (2015) 1199-1207.
26. L.A.E. Wang, A.M.V. Gomez, E.M.A. Estrada, A.M. Robledo, *Electrochim. Acta* 112 (2013) 164-170.
27. G.H. Song, M.Q. Shi, Y.Q. Chu, C.A. Ma, *Electrochim. Acta* 112 (2013) 53-58.
28. E. Lam, J.H.T. Luong, *ACS catalysis* 4 (2014) 3393-3410.
29. H. Razmi, E. Habibi, H. Heidari, *Electrochim. Acta* 53 (2008) 8178-8185.
30. A.S. Aarnio, M. Borghei, I.V. Anoskin, A.G. Nasibulin, E.I. Karuppinen, V. Ruiz, T. Kallio, *Int. J. Hydrogen Energy* 37 (2012) 3415-3424.
31. J.R.C. Salgado, V.A. Paganin, E.R. Gonzalez, M.F. Montemor, I. Tacchini, A. Anson, M.A. Salvador, P. Ferreira, F.M.L. Figueiredo, M.G.S. Ferreira, *Int. J. Hydrogen Energy* 38 (2013) 910-920.
32. J. Zeng, C. Francia, C. Gerbaldi, V. Baghio, S. Specchia, A.S. Arico, P. Spinelli, *Electrochim. Acta* 94 (2013) 80-91.
33. H. Wang, R. Wang, H. Li, Q. Wang, J. Kang, Z. Lei, *Int. J. Hydrogen Energy* 36 (2011) 839-848.
34. E. Salernitano, L. Giorgi, T.D. Markis, *Int. J. Hydrogen Energy* 39 (2014) 15005-15016.
35. M. Noroozifar, M.K. Motlagh, M.S.E. Kakhki, R.K. Moghadam, *J. Power Sources* 248 (2014) 130-139.
36. M.C. Tsai, T.K. Yeh, C.H. Tsai, *Int. J. Hydrogen Energy* 36 (2011) 8261-8266.
37. N. Jha, R.I. Jafri, N. Rajalakshmi, S. Ramaprabhu, *Int. J. Hydrogen Energy* 36 (2011) 7284-7290.
38. Y. Zhao, X. Yang, J. Tian, F. Wang, L. Zhan, *Int. J. Hydrogen Energy* 35 (2010) 3249-3257.
39. X. Yang, X. Wang, G. Zhang, J. Zheng, T. Wang, X. Liu, C. Shu, L. Jiang, C. Wang, *Int. J. Hydrogen Energy* 37 (2012) 11167-11175.
40. G. Yang, X. Yang, M. Xu, C. Min, H. Xiao, K. Jiang, L. Chen, G. Wang, *J. Power Sources* 222 (2013) 340-343.
41. G. Girishkumar, T.D. Hall, K. Vinodgopal, P.V. Kamat, *J. Phys. Chem. B* 110 (2006) 107-114.
42. M. Zhang, J. Xie, Q. Sun, Z. Yan, M. Chen, J. Jing, *Int. J. Hydrogen Energy* 38 (2013) 16402-16409.
43. Y. Zhang, H. Shu, G. Chang, K. Ji, M. Oyama, X. Liu, Y. He, *Electrochim. Acta* 109 (2013) 570-576.
44. Y. Huang, H. Huang, Q. Gao, C. Gan, Y. Liu, Y. Fang, *Electrochim. Acta* 149 (2014) 34-41.
45. Z. Wang, G. Shi, J. Xia, Y. Xia, F. Zhang, L. Xia, D. Song, J. Liu, L. Xia, M.E. Brito, *Electrochim. Acta* 121 (2014) 245-252.
46. S. Yu, Q. Liu, W. Yang, K. Han, Z. Wang, H. Zhu, *Electrochim. Acta* 94 (2013) 245-251.
47. C. Zhai, M. Zhu, D. Bin, H. Wang, Y. Du, C. Wang, P. Yang, *ACS Appl. Mater. Interfaces* 6 (2014) 17753-17761.
48. F. Jiang, F. Ren, W. Zhou, Y. Du, J. Xu, P. Yang, C. Wang, *Fuel* 102 (2012) 560-566.
49. H. Gao, J.B. He, Y. Wang, N. Deng, *J. Power Sources* 205 (2012) 164-172.
50. Z. Wang, G. Gao, H. Zhu, Z. Sun, H. Liu, X. Zhao, *Int. J. Hydrogen Energy* 34 (2009) 9334-9340.
51. K.R. Knowles, C.C. Honson, A.L. Fogel, B. Warhol, D.A. Rider, *ACS Appl. Mater. Interfaces* 4 (2012) 3575-3583.
52. W. Zhou, Y. Du, F. Ren, C. Wang, J. Xu, P. Yang, *Int. J. Hydrogen Energy* 35 (2010) 3270-3279.

53. B. Habibi, M.H.P. Azar, *Int. J. Hydrogen Energy* 35 (2010) 9318-9328.
54. S. Ghosh, A.L. Teillout, D. Floresyona, P.D. Oliveira, A. Hagege, H. Remita, *Int. J. Hydrogen Energy* 40 (2015) 4951-4959.
55. H. Sun, X. Jiao, H. Wang, Z. Jiang, D. Chen, *ACS Appl. Mater. Interfaces* 3 (2011) 2425-2430.
56. R. Gupta, S.K. Guin, S.K. Aggarwal, *Electrochim. Acta* 116 (2014) 314-320.
57. Z. Yan, H. Wang, M. Zhang, Z. Jiang, T. Jiang, J. Xie, *Electrochim. Acta* 95 (2013) 218-224.
58. E.N.E. Sawy, H.M. Molero, V.I. Birss, *Electrochim. Acta* 117 (2014) 202-210.
59. Z. Yao, R. Yue, C. Zhai, F. Jiang, H. Wang, Y. Du, C. Wang, P. Yang, *Int. J. Hydrogen Energy* 38 (2013) 6368-6376.
60. S.P. Lim, A. Pandikumar, N.M. Huang, H.N. Lim, *Int. J. Hydrogen Energy* 39 (2014) 14720-14729.
61. S.R. Hosseini, J.B. Raoof, S. Ghasemi, Z. Gholami, *Int. J. Hydrogen Energy* 40 (2015) 292-302.
62. J.U. Godinez, V.G. Montalvo, O.J. Sandoval, *Int. J. Hydrogen Energy* 39 (2014) 9121-9127.
63. C.T. Hsieh, J.Y. Lin, *J. Power Sources* 188 (2009) 347-352.
64. Y. Peng, C. Liu, C. Pan, L. Qiu, S. Wang, F. Yan, *ACS Appl. Matter. Interfaces* 5 (2013) 2752-2760.
65. L. Giorgi, E. Salernitano, T.D. Makris, S. Gagliardi, V. Contini, M.D. Francesco, *Int. J. Hydrogen Energy* 39 (2014) 21601-21612.
66. Y. Zhang, G. Chang, H. Shu, M. Oyama, X. Liu, Y. He, *J. Power Sources* 262 (2014) 279-285.
67. Y. Wang, Y. Zhao, J. Yin, M. Liu, Q. Dong, Y. Su, *Int. J. Hydrogen Energy* 39 (2014) 1325-1335.
68. Q. Dong, Y. Zhao, X. Han, Y. Wang, M. Liu, Y. Li, *Int. J. Hydrogen Energy* 39 (2014) 14669-14679.
69. P.C. Biswas, T. Ohmori, M. Enyo, *J. Electroanal. Chem*. 305 (1991) 205-215.
70. H. Huang, Y. Liu, Q. Gao, W. Ruan, X. Lin, X. Li, *ACS Appl. Mater. Interfaces* 6 (2014) 10258-10264.
71. Y. Zhao, R. Wang, Z. Han, C. Li, Y. Wang, B. Chi, J. Li, X. Wang, *Electrochim. Acta* 151 (2015) 544-551.
72. J. Masud, M.T. Alam, Z. Awaludin, M.S.E. Deab, T. Okajima, T. Ohsaka, *J. Power Sources* 220 (2012) 399-404.
73. A. Nouralishahi, A.A. Khodadadi, Y. Mortazovi, A. Rashidi, M. Choolaei, *Electrochim. Acta* 147 (2014) 192-200.
74. Y. Huang, H. Huang, Q. Gao, C. Gan, Y. Liu, Y. Fang, *Electrochim. Acta* 149 (2014) 34-41.
75. J. Zeng, C. Francia, C. Gerbaldi, V. Baglio, S. Specchia, A.S. Arico, P. Spinelli, *Electrochim. Acta* 94 (2013) 80-91.
76. K. Scott, A.K. Shukla, C.L. Jackson, W.R.A. Mealeman, *J. Power Sources* 126 (2004) 67-75.
77. X. Yang, Y. Liu, Y. Feng, L. Wang, S. Li, W. Wei, *J. Power Sources* 234 (2013) 272-276.
78. G.C. Manrique, A.V. Palenzuela, E. Brillas, F. Centellas, J.A. Garrido, R.M. Rodriquez, P.L. Cabot, *Int. J. Hydrogen Energy* 39 (2014) 12859-12869.
79. M. Higa, S. Feng, N. Endo, Y. Kakihana, *Electrochim. Acta* 153 (2015) 83-89.
80. M. Higa, K. Hatemura, M. Sugita, S.I. Maesowa, M. Nishimura, N. Endo, *Int. J. Hydrogen Energy* 37 (2012) 6292-6301.
81. N. Katiyar, S. Kumar, S. Kumar, *J. Power Sources* 243 (2013) 381-391.
82. H. Zhao, J. Yang, L. Li, H. Li, J. Wang, Y. Zhang, *Int. J. Hydrogen Energy* 34 (2009) 3908-3914.
83. W. Zhou, Y. Du, F. Ren, C. Wang, J. Xu, P. Yang, *Int. J. Hydrogen Energy* 35 (2010) 3270-3279.
84. J. Qian, W. Wei, H. Huang, Y. Tao, K. Chen, X. Tang, *J. Power Sources* 210 (2012) 345-349.
85. F. Ren, C. Zhai, M. Zhu, C. Wang, H. Wang, D. Bin, J. Guo, P. Yang, Y. Du, *Electrochim. Acta* 153 (2015) 175-183.

86. H. He, P. Xiao, M. Zhou, Y. Zhang, Q. Lou, X. Dong, *Int. J. Hydrogen Energy* 37 (2012) 4967-4973.
87. Y. Hao, Y. Yang, L. Hong, J. Yuan, L. Niu, Y. Gui, *ACS Appl. Mater. Interfaces* 6 (2014) 21986-21994.
88. Y.K. Su, H. Liu, M. Feng, Z.L. Yan, Z.H. Cheng, J.N. Tang, H.T. Yang, *Electrochim. Acta* 161 (2015) 124-128.
89. J. Prabhuram, N. Nambikrishnan, B. Choi, T.H. Lim, H.Y. Ha, S.K. Kim, *Int. J. Hydrogen Energy* 35 (2010) 6924-6933.
90. J. Zang, Y. Wang, L. Bian, J. Zhang, F. Meng, Y. Zhao, X. Qu, S. Ren, *Int. J. Hydrogen Energy* 37 (2012) 6349-6355.
91. Y. Liu, D. Li, V.R. Stamenkovic, S.S. Soled, J.D. Henao, S. Sun, *ACS Catal.* 1 (2011) 1719-1723.
92. R.I. Jafri, N. Rajalakshmi, K.S. Dhathathreyan, S. Ramaprabhu, *Int. J. Hydrogen Energy* 40 (2015) 4337-4348.
93. L.P.R. Profeti, D. Profeti, P. Olivi, *Int. J. Hydrogen Energy* 34 (2009) 2747-2757.
94. X. Chen, C. Si, Y. Gao, J. Frenzel, J. Sun, G. Eggeler, Z. Zhang, *J. Power Sources* 273 (2015) 324-332.
95. T.Y. Wu, B.K. Chen, J.K. Chang, P.R. Chen, C.W. Kuo, *Int. J. Hydrogen Energy* 40 (2015) 2631-2640.
96. J.M. Jehng, W.J. Liu, T.C. Pan, Y.M. Dai, *Appl. Surf. Sci.* 268 (2013) 425-431.
97. X. Chen, Y. Jiang, J. Sun, C. Jin, Z. Zhang, *J. Power Sources* 267 (2014) 212-218.
98. H. Gharibi, K. Kakaei, M. Zhiani, M.M. Taghiabadi, *Int. J. Hydrogen Energy* 36 (2011) 13301-13309.
99. D. Ruan, F. Gao, Z. Guo, *Electrochim. Acta* 147 (2014) 225-231.
100. J.M. Sieben, A.E. Alvarez, V. Comignani, M.M.E. Duarte, *Int. J. Hydrogen Energy* 39 (2014) 11547-11556.
101. R. Ding, L. Qi, M. Jia, H. Wang, *J. Power Sources* 251 (2014) 287-295.
102. L. Zhang, A. Gao, Y. Liu, Y. Wang, J. Ma, *Electrochim. Acta* 132 (2014) 416-422.
103. Y. Zhang, R. Zhu, Y. Cui, J. Zhong, X. Zhang, J. Chen, *Nanotechnology* 25 (2014) 135607.
104. H. Huang, S. Yang, R. Vajtai, X. Wang, P.M. Ajayan, *Adv. Mater*., 26 (2014) 5160-5165.
105. J.J. Shao, Z.J. Li, C. Zhang, L.F. Zhang, Q.H. Yang, *J. Mater. Chem*. A 2 (2014) 1940-1946.
106. M. Yang, R. Guarecuco, F.J. Disalvo, *Chem. Mater*. 25 (2013) 1783-1787.
107. Y. Liu, M .Chi, V. Mazumder, K.L. More, S. Soled, J.D. Henao, S. Sun, *Chem. Mater*. 23 (2011) 4199-4203.
108. H. Gharibi, M. Amani, H. Pahalavanzadeh, M. Kazemeini, *Electrochim. Acta* 97 (2013) 216-225.
109. F. Miao, B. Tao, *Electrochim. Acta* 56 (2011) 6709-6714.
110. F. Xie, H. Meng, P.K. Shen, *Electrochim. Acta* 53 (2008) 5039-5044.
111. J.S. Cooper, P.J.M. Ginn, *J. Power Sources* 163 (2006) 330-338.
112. M. Inoue, T. Iwasaki, M. Umeda, *Int. J. Hydrogen Energy* 38 (2013) 8992-8999.
113. H. Yuan, D. Guo, X. Qiu, W. Zhou, L .Chen, *J. Power Sources* 188 (2009) 8-13.
114. E. Capitanio, S. Siracusano, A. Stassi, V. Baglio, A.S. Arico, A.C. Tavares, *Int. J. Hydrogen Energy* 39 (2014) 8026-8033.
115. D. Chateraborty, I. Chorkendorff, T. Johannessen, *J. Power Sources* 162 (2006) 1010-1022.
116. Z.B. Wang, G.P. Yin, Y.Y. Shao, B.Q. Yang, P.F. Shi, P.X. Feng, *J. Power Sources* 165 (2007) 9-15.
117. S.H. Seo, C.S. Lee, *Energy & Fuels* 22 (2008) 1204-1211.
118. M. Chen, C.Y. Du, G.P. Yin, P.F. Shi, T.S. Zhao, *Int. J. Hydrogen Energy* 34 (2009) 1522-1530.
119. G. Girishkumar, K. Vinodgopal, P.V. Kamat, *J. Phys. Chem. B* 108 (2004) 19960-19966.
120. B. Narayanamoorthy, K.K.R. Datta, M. Eswaramoorthy, S. Balaji, *ACS Catalyst* 4 (2014) 3621-3629.

121. J. Luo, P.N. Njoki, Y. Lin, D. Mott, L. Wang, C.J. Zhong, *Langmuir* 22 (2006) 2892-2898.
122. A.V. Palenzuela, F. Centellas, J.A. Garrido, C. Arias, R.M. Rodriquez, E. Brillas, P.C. Cabot, *J. Power Sources* 196 (2011) 3503-3512.
123. A.S. Gonzalez, E.B. Arco, J. Escalante, O.J. Sandoval, S.A. Gomboa, *Int. J. Hydrogen Energy* 37 (2012) 1752-1759.
124. E. Teliz, V. Diaz, C.F. Zinola, *Electrochim. Acta* 125 (2014) 556-565.
125. F. Chen, S. Zhou, G. Ji, K. Sundmacher, C. Zhang, *Int. J. Hydrogen Energy* 34 (2009) 5563-5567.
126. M.M. Bruno, M.A. Petruccelli, F.A. Viva, H.R. Corti, *Int. J. Hydrogen Energy* 38 (2013) 4116-4123.
127. Y. Kang, J.B. Pyo, X. Ye, T.R. Gorden, C.B. Murray, *ACS Nano* 6 (2012) 5642-5647.
128. T. Yang, *Int. J. Hydrogen Energy* 34 (2009) 6917-6924.
129. C. Yang, J. Wang, X. Xie, S. Wang, Z. Mao, H. Wang, *Int. J. Hydrogen Energy* 37 (2012) 867-872.
130. N. Jha, A.L.M. Reddy, M.M. Shaijumon, N. Rajalakshmi, S. Ramaprabhu, *Int. J. Hydrogen Energy* 33 (2008) 427-433.
131. S. Zhou, S. Wang, Y. Gao, L. Jiang, H. Sun, G. Sun, *Int. J. Hydrogen Energy* 35 (2010) 11254-11260.
132. D. You, Y. Lee, H. Cho, J.H. Kim, C. Pak, G. Lee, K.Y. Park, J.Y. Park, *Int. J. Hydrogen Energy* 36 (2011) 5096-5103.
133. S. Chen, F. Ye, W. Lin, *Int. J. Hydrogen Energy* 35 (2010) 8225-8233.
134. G.K.S. Prakash, F.C. Krause, F.A. Viva, S.R. Narayaan, G.A. Ola, *J. Power Sources* 196 (2011) 7967-7972.
135. H.C. Chien, L.D. Tsai, C.P. Huang, C.Y. Kang, J.N. Lin, F.C. Chang, *Int. J. Hydrogen Energy* 38 (2013) 13792-13801.
136. S.S. Araya, I.F. Grigoras, F. Zhou, S.J. Andreasen, S.K. Koer, *Int. J. Hydrogen Energy* 39 (2014) 18343-18350.
137. Q. Jiang, L. Jiang, H. Hou, J. Qi, S. Wang, G. Sun, *J. Phys. Chem. C* 114 (2010) 19714-19722.
138. M. Das, L. Barbora, P. Das, P. Goswami, *Biosens. Bioelectron.* 59 (2014) 184-191.
139. M.M.H. Sadrabadi, E. Dashtimoghandam, N. Mokarram, F.S. Majedi, K.I. Jacob, *Polymer* 53 (2012) 2643-2651.
140. S. Dutta, C. Ray, A. Mondel, S.K. Mahetor, S. Sarkar, T. Pal, *Electrochim. Acta* 159 (2015) 52-60.
141. T. Arikan, A.M. Kannan, F. Kadirgan, *Int. J. Hydrogen Energy* 38 (2013) 2900-2907.
142. V. Baglio, D. Sebastian, C.D. Urso, A. Stassi, R.S. Amin, K.M.E. Khatib, A.S. Arico, *Electrochim. Acta* 128 (2014) 304-310.
143. Q.X. Wu, T.S. Zhao, *Int. J. Hydrogen Energy* 36 (2011) 5644-5654.
144. M.L Faro, A. Stassi, V. Antonucci, V. Modafferi, P. Frontera, P. Antonucci, A.S. Arico, *Int. J. Hydrogen Energy* 36 (2011) 9977-9986.